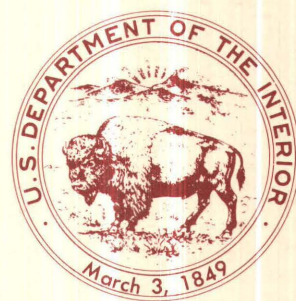


A Study of Rock Stresses and Engineering Geology in Quarries of the Barre Granite of Vermont

U.S. GEOLOGICAL SURVEY BULLETIN 1593



A Study of Rock Stresses and Engineering Geology in Quarries of the Barre Granite of Vermont

By Thomas C. Nichols, Jr.

U.S. GEOLOGICAL SURVEY BULLETIN 1593

DEPARTMENT OF THE INTERIOR
DONALD PAUL HODEL, *Secretary*

U.S. GEOLOGICAL SURVEY
Dallas L. Peck, Director



UNITED STATES GOVERNMENT PRINTING OFFICE, WASHINGTON: 1986

For sale by the Branch of Distribution
Books and Open-File Reports Section
U.S. Geological Survey
Federal Center
Box 25425
Denver, CO 80225

Library of Congress Cataloging in Publication Data

Nichols, Jr., Thomas C.

A study of rock stresses and engineering geology in quarries of the Barre granite of Vermont.
(U.S. Geological Survey bulletin ; 1593)

Bibliography: p.

Supt. of Docs. No.: I 19.3:1593

1. Rock mechanics—Vermont—Barre Region. 2. Engineering geology—Vermont—Barre Region. 3. Granite industry and trade—Vermont—Barre Region.

I. Title. II. Series.

QE75.B9 no. 1593

[TA706.5]

557.3 s

[624.1'51'097434]

85-600205

CONTENTS

Abstract	1
Introduction	1
Acknowledgments	1
In situ stress investigations, Barre, Vermont	1
Objectives and methods	1
Geologic setting	2
Geology of the Barre Granite	3
Origin and age	3
Structure	3
Modal composition and petrofabrics	6
Site selection	8
Deformation, stress, and temperature measurements	8
Type of measurement and locations	9
Results of temperature measurements	10
Prequarrying stresses	12
Overcore measurements	13
Measured prequarry stresses compared to predicted gravity stresses	17
Stress changes and surface deformations caused by quarrying	17
Time-dependent deformation of cores	19
Elastic modulus determinations	21
Discussion of results	23
Measurements indicative of inelastic-rock response stress	24
Local distribution of determined vertical and horizontal stress	24
Influence of geologic features on determined stress distribution	25
Fractures and faults	26
Evidence for influence of geologic history	26
Fabric	27
Mechanical behavior characteristics—results of quarrying	28
Relief characteristics	28
Modulus	28
Significance of Barre data to quarrying and engineering practice	29
Conclusions	30
References	30

FIGURES

1. Map showing location of report area adjacent to Barre, Vt. 2
2. Photographs of working area in Wetmore and Morse quarry, Barre, Vt. 2
3. Map showing area of outcropping Barre Granite southeast of Barre, Vt. 3
4. Topographic map of the upper and lower quarry areas showing shear zones along granite-metamorphic boundary 4
5. Equal-area diagrams of poles to natural fractures mapped in the lower and upper quarry areas at Barre, Vt. 5
- 6–10. Photographs showing:
 6. Tendency of sheeting fractures developed in upper quarry area to terminate at boundaries of older fractures 6
 7. Very extensive but widely spaced northwest-trending fractures found in the upper quarry area 7
 8. Well-developed northeast-trending shear zones found in the interior portion of the pluton, lower quarry area 7

9. Well-developed northeast-trending fracture and shear zones terminate abruptly at massive unfractured granite of upper quarry area **8**
10. Open and healed microcracks in quartz crystals, Barre Granite **9**
11. Perspective view of 10×10×5.7-m block of Barre Granite and adjacent quarry area, Wetmore and Morse quarry, showing locations of boreholes and sheeting fractures **10**
12. Isometric view of 10×10×5.7-m block of Barre Granite showing borehole, overcore, and hydrofracture locations and section views of the same block showing locations of prequarry and postquarry measurements **11**
13. Schematic diagram showing locations of displacement deformation nets 1, 2, 2E, 3, and 4, Wetmore and Morse quarry **12**
14. Graph showing measured temperature versus time in 10×10×5.7-m block and adjacent rock **13**
15. Plot of secondary maximum principal stress magnitudes measured on the block versus maximum distance of stress measurement location from known fractures **15**
16. Equal-area diagrams showing orientations of principal stresses determined within 10×10×5.7-m block of Barre Granite **16**
17. Gravity stresses determined by a plane-strain finite-element calculation in the vertical plane AB **18**
18. Graphs showing displacements versus time for nets 1, 2, 2E, and 3 after the 10×10×5.7-m block of Barre Granite was quarried **19**
19. Photograph showing diskings of 5.7-cm-diameter cores retrieved from hole 5 drilled after the 10×10×5.7-m block was quarried **21**
- 20–24. Graphs showing:
 20. Extensional strains measured through time on exterior of overcore annuli after extraction from borehole **21**
 21. Strains occurring through time on a 5-cm core after extraction from drill hole 1a in 10×10×5.7-m block **22**
 22. Variation of static Young's modulus in the horizontal plane, unquarried block of Barre Granite **23**
 23. Variation of static Young's modulus in vertical planes striking N. 50° W. and N. 40° E., unquarried block of Barre Granite **24**
 24. Variation of static Young's modulus in the horizontal plane, large quarried Barre Granite block **25**
25. Vertical section through hole 2H showing locations of overcores and a natural fracture **26**
26. Photographs showing fractures at edges of partially freed granite blocks (A), and in bottom of quarry (B), Barre, Vt. **29**

TABLES

1. Determinations of stresses made on Barre Granite adjacent to and within the 10×10×5.7-m block prior to and after quarrying, Wetmore and Morse quarry **14**
2. Measured and gravity stresses in the x, y, and z directions in Barre Granite **17**
3. Internal radial borehole displacements for typical overcore samples through specified time intervals, Barre Granite **21**
4. Young's moduli determined on cores of Barre Granite by sonic-pulse methods **26**

A Study of Rock Stresses and Engineering Geology in Quarries of the Barre Granite of Vermont

By Thomas C. Nichols, Jr.

Abstract

In situ stress studies in granite quarries of the Rock of Ages Corporation near Barre, Vermont, have revealed that:

1. Apparent local in situ stress distribution is strongly affected by geologic structure and rock outcrop geometry.
2. Geologic history and paleostress fields may in part be responsible for the determined local stress distributions and rock anisotropies.
3. Measured stress changes caused by rock quarrying are nearly equivalent to the stresses measured prior to quarrying; that is, quarrying relieves virtually all stress.
4. Extensional failures, detrimental to efficient rock extraction, that occurred as a result of quarrying and coring are difficult to explain by commonly used failure criteria.
5. Rebound deformations observed in the quarries that are detrimental to the quarrying occur as both rapid and time-dependent deformations. Nearly instantaneous deformations measured on surface grids are in good agreement with the measured stress relief caused by quarrying. Additional short-term, time-dependent deformations were nearly the same as the initial deformations. However, there is reason to doubt that the initial rapid deformations used for the interpretation of stresses are elastic. If they are a result of inelastic microfracture opening, the stress interpretations may be in considerable doubt.

For engineering purposes, these studies demonstrate that the levels and distribution of local in situ stress and the rock response resulting from engineering excavation may be difficult to adequately assess without making sufficient and meaningful in situ geotechnical measurements.

INTRODUCTION

The experiment described herein was an attempt to evaluate the state of stress and mechanical rock behavior caused by excavation at shallow depths in an outcropping

crystalline quarry rock, the Barre Granite of Vermont. In addition, it was hoped that the information obtained would aid the quarry operation in developing more efficient quarrying procedures in locations where unloading failures damage good quarry rock. The distribution of elastic properties, stress magnitudes, and orientations was compared to geologic structures, quarry procedures, outcrop geometry, and quarry history in an effort to determine their relationship. Finally, an attempt was made to evaluate the relief behavior of the granite by observing deformations and associated stress changes caused by quarrying a large block in the area of the investigation.

Acknowledgments

I wish to thank John F. Abel, Jr., of the Colorado School of Mines for his timely and helpful discussion concerning the technical aspects covered in this report. In addition, I wish to thank the Rock of Ages Corp. of Vermont for their generous cooperation and for letting us use their facilities for conducting the field experiments.

IN SITU STRESS INVESTIGATIONS, BARRE, VERMONT

Objectives and Methods

At Barre, Vt. (fig. 1), the U.S. Geological Survey (USGS) conducted a field experiment in the Barre Granite, a pluton of Devonian age, to determine the nature and variation of the stress and strain fields within a large (10×10×5.7-m) granite block prior to and as a result of quarrying (Nichols and others, 1977). The objectives were to (1) locally determine and map geologic and other physical features that may influence the local stress field, (2) determine the prequarrying and postquarrying stress fields, and (3) on cored samples, conduct laboratory physical-properties tests necessary to interpret field tests.

Conventional deformation measurements, undercoring, overcoring, and hydrofracturing techniques were used



Figure 1. Location of report area (shaded) adjacent to Barre, Vt.

to investigate the stress and strain response of the block and the surrounding rock that occurred as a result of quarrying operations. The block investigated was in the Wetmore and Morse quarry, owned by the Rock of Ages Corp., and exposed at a depth of 67 m below the original ground surface (fig. 2). The investigations included mapping the block and surrounding rock to record the geologic and geometric features. Locally, these were mainly sheet joints, other natural and quarry-associated fracture systems, fabric anisotropies herein called the “rift, grain or lift, and hardway planes,” and the configuration of the quarry. The “rift” is the plane of easiest rock splitting, the “grain or lift” is the second easiest plane of splitting, and the “hardway” is the most difficult plane of splitting. According to the quarry operator, in the vicinity of our measurements, the rift is nearly vertical and strikes N. 40° E., the lift is horizontal, and the hardway is vertical, striking N. 50° W.

Geologic Setting

The geology of the area and detailed investigations of the Vermont granites have been described by various workers. Dale (1909) published a comprehensive report on the structural and physical aspects of commercial granites in New England, which included the Barre Granite.

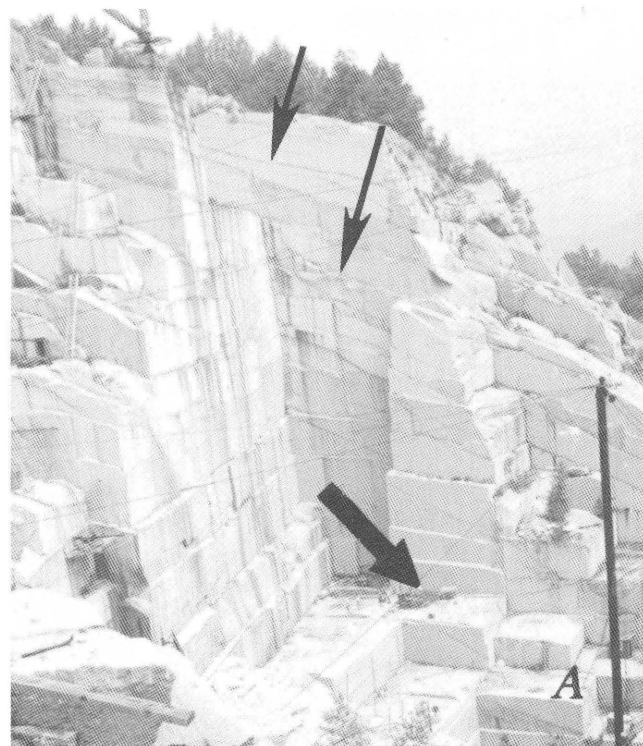


Figure 2. Working area in Wetmore and Morse quarry, Barre, Vt. *A*, View to the north. Large arrow designates 10×10×5.7-m Barre Granite block prior to quarrying. Sheet fractures dip southeast (small arrows). *B*, Closeup of block showing sheet (large arrows) and other fractures (small arrows).

Balk (1937) made a detailed study of structural relations in the Barre Granite and other granitic plutons. White and Jahns (1950) published a description of structural relations in central Vermont. Stratigraphic studies have been made in the area by Currier and Jahns (1941), Doll (1943), and Cady (1960). Petrographic studies of the Barre Granite have been conducted by Finlay (1902) and Chayes (1952). A report by Murthy (1957), in which he mapped and described the bedrock geology of the East Barre, Vt., quadrangle, is used as the geologic basis for this report.

The term Barre Granite as used here refers to a granite body that crops out in a bifurcated, somewhat elliptical shape (fig. 3) about 2 km southeast of Barre, Vt. The outcropping body is about 7.1 km long, and 3.0 km wide, with the long axis trending about N. 28° E. Most of the Barre Granite is bounded by the Silurian Westmore Formation (Doll, 1951); a small portion of the northeast boundary is in contact with the younger Waits River Formation, also of Silurian age.

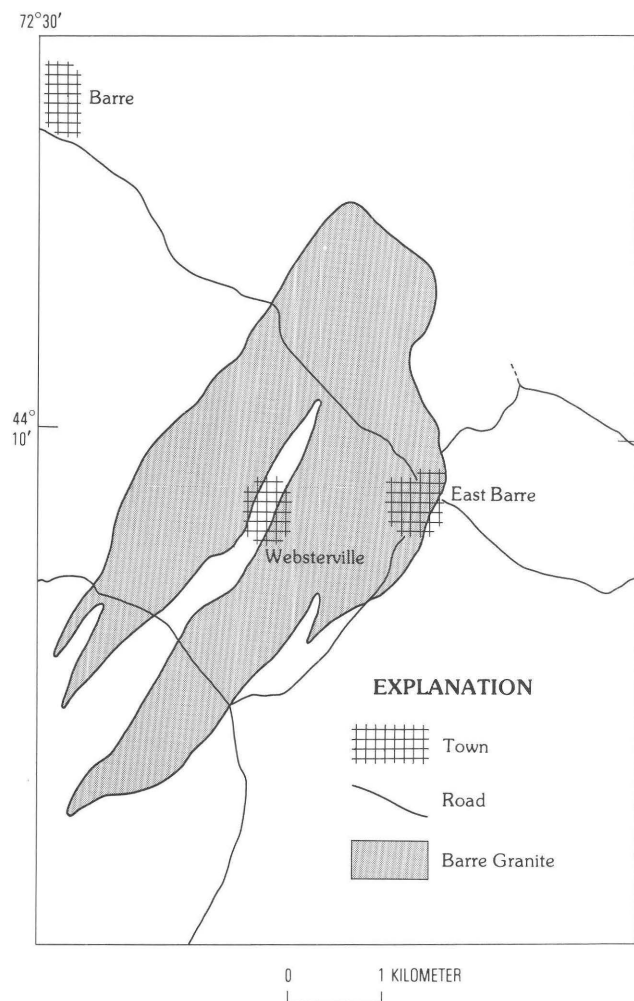


Figure 3. Area of outcropping Barre Granite southeast of Barre, Vt.

The Westmore Formation consists primarily of various interbedded micaceous and quartzose schists with individual beds from 8 to 30 cm thick. The total thickness of the formation varies from 0.9 to 1.2 km. The mica schists in the westernmost outcrops become progressively more quartzose to the east. Local porphyroblasts of garnet and biotite occur in the mica schists, and garnet porphyroblasts are quite common in the micaceous beds interbedded with more quartzose lithologies.

The Waits River Formation consists primarily of calcareous rocks with interbedded mica schists and is estimated to have a thickness of about 1.5–2.0 km.

Geology of the Barre Granite

Origin and Age

The Barre Granite is thought to be an intrusive body concordant on a regional scale but discordant at local contacts. The mode of emplacement probably consisted of both passive intrusion along zones of structural weakness and forcible intrusion accompanied by the stoping process. The intrusion of Barre-type granite plutons is thought to have occurred $377\text{--}383 \times 10^6$ years ago (Naylor, 1971), postdating the regional metamorphism of the Devonian Acadian orogeny. Zartman and others (1970) suggest that the plutons may have cooled slowly as a result of continued burial by upper Paleozoic sediments. This may explain the younger K-Ar ages of $340\text{--}349 \times 10^6$ years determined for granites obtained in the Rock of Ages quarry near Barre and the Adamant quarry to the northwest (Faul and others, 1963). High-grade thermal metamorphism (Murthy, 1957) was superposed on the previously metamorphosed Westmore and Waits River Formations at the contact with the Barre Granite, indicating that these rocks must have been altered at temperatures of at least $400\text{--}500^\circ\text{C}$ and probably were under moderately deep to shallow overburden. The depth of burial was estimated to be about 10 km (Nichols, 1980).

Structure

Dale (1923) described in detail the major fracture sets that exist in the active quarries on the Barre Granite pluton. He noted that in 26 quarries the most frequent joints strike N. $30^\circ\text{--}40^\circ$ E. and N. $75^\circ\text{--}90^\circ$ E., the next most frequent strike N. $60^\circ\text{--}70^\circ$ E., N. $30^\circ\text{--}40^\circ$ W., and N. $10^\circ\text{--}25^\circ$ W. Dale also noted that the rift plane was reported to be vertical but varied in strike from N. 30° E. to N. 75° E., and that the grain plane was horizontal in most areas. Murthy (1957) observed that the most conspicuous joint set trends approximately N. 20° E. and dips between 45° and 80° to the southwest. He asserts that

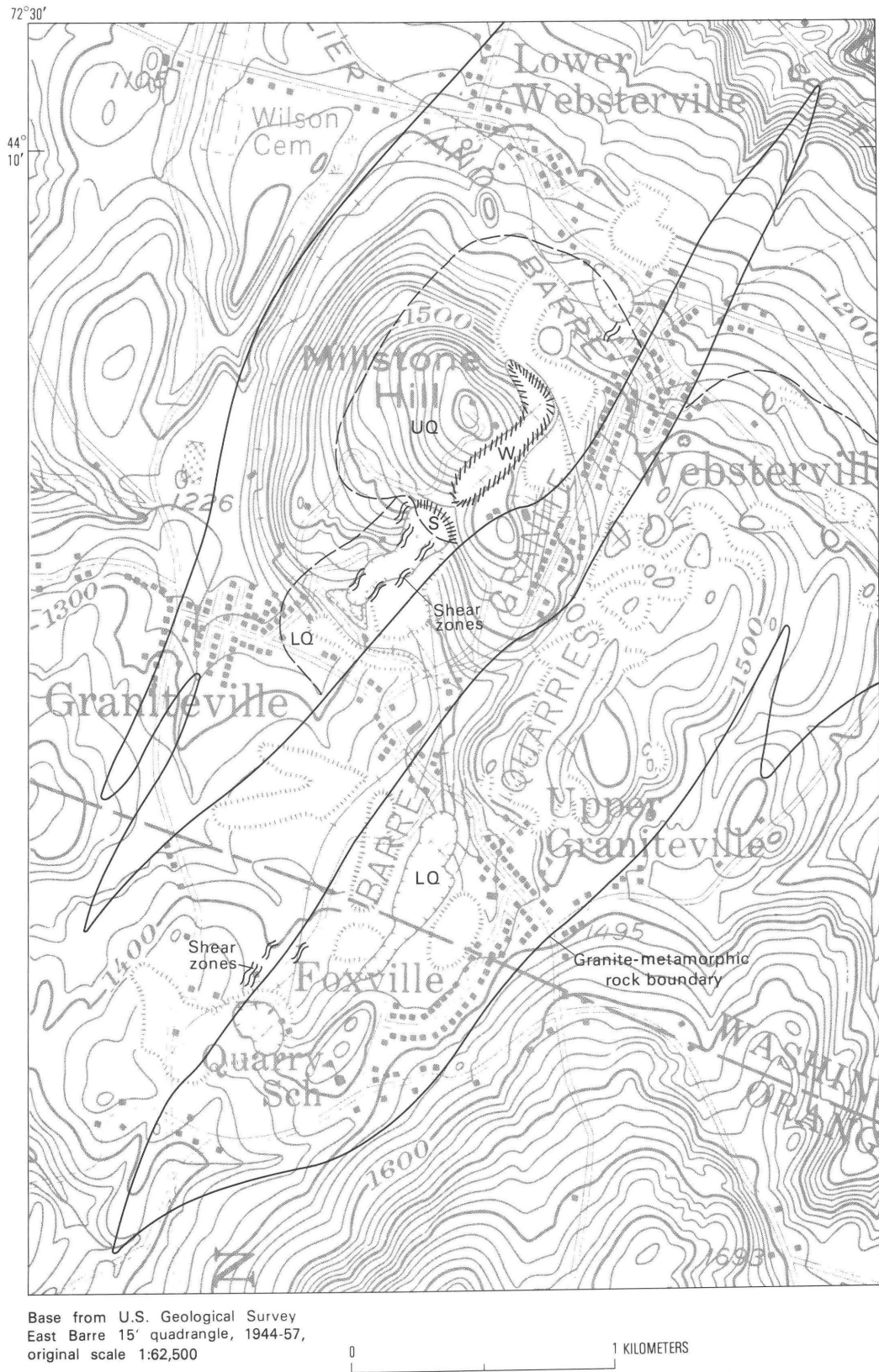


Figure 4. Topographic map of the upper and lower quarry areas showing shear zones along granite-metamorphic boundary. Dashed lines define approximate location of lower (LQ) and upper (UQ) quarry areas in the granite. Hachures outline the Upper Smith and Weston (S) and the Wetmore and Morse (W) quarries.

these fractures are parallel to the rift direction and trend of the flow lines.

Fractures were mapped by the author in both active and abandoned quarries to determine if fractures described by Dale may vary areally in any systematic way. The fracture pattern and density in the south and east sections of the pluton differ significantly from those in the west-central section. The south and east sections of the pluton are topographically lower than the west-central section by at least 30 m; hence, quarries in the high areas are referred to as the upper quarries (UQ, fig. 4) and those in the low areas as the lower quarries (LQ, fig. 4). Figure 5 shows comparative orientations of fracture systems in these two areas.

The west-central part of the pluton, in which the Upper Smith and Weston and the Wetmore and Morse quarries (fig. 4) are located, has two strong sets of fractures that appear to be almost nonexistent to the south and east in the lower quarries. These are the near-surface, well-developed, low-angle sheeting fractures (cluster a, fig. 5A, and fig. 6) and the very extensive northwest-trending nearly vertical fractures (cluster b, fig. 5A). Nearly closed sheeting fractures with spacings commonly <0.3 m are thought to be nontectonic in origin and probably occur as a result of vertical stress relief caused by denudation. The northwest-trending fractures, probably of tectonic origin, are usually single fractures <0.5 cm thick and are widely spaced, but may extend laterally hundreds of meters (fig. 7). These fractures have vertical slickensides superposed on hydrothermal alteration products, in some locations mostly illite. Although the displacement on the fractures is very small, the sense of movement as evidenced by feather fractures is that of high-angle reverse faulting. Toward the surface of the pluton, the vertical fractures tend to bifurcate and curve into a horizontal direction. The deepest sheeting fractures tend to inter-finger and intersect the bifurcated fractures and in many places have a similar dip; thus, the two sets can easily be confused.

The lower quarries (fig. 4) contain a pervasive set of well-developed, steeply dipping, northeast-trending fractures (fig. 5B). These are strongly developed fractures that are subparallel to the long axis of the pluton and the regional trend of the surrounding country rocks. They grade into broad, well-developed shear zones (figs. 8, 9), found along the granite-metamorphic contacts interior to both of the pluton's southern segments (fig. 4), and terminate abruptly as they extend northward into the upper quarries (figs. 4, 9). The northeast-trending fracture set tends to extend into and through the upper quarry area only immediately adjacent to the contact with the metamorphic rocks, and here the set is not nearly as well developed as in the lower quarries. These fractures also are intruded by basic and felsic dikes and are filled with hydrothermal alteration products. Murthy (1957) con-

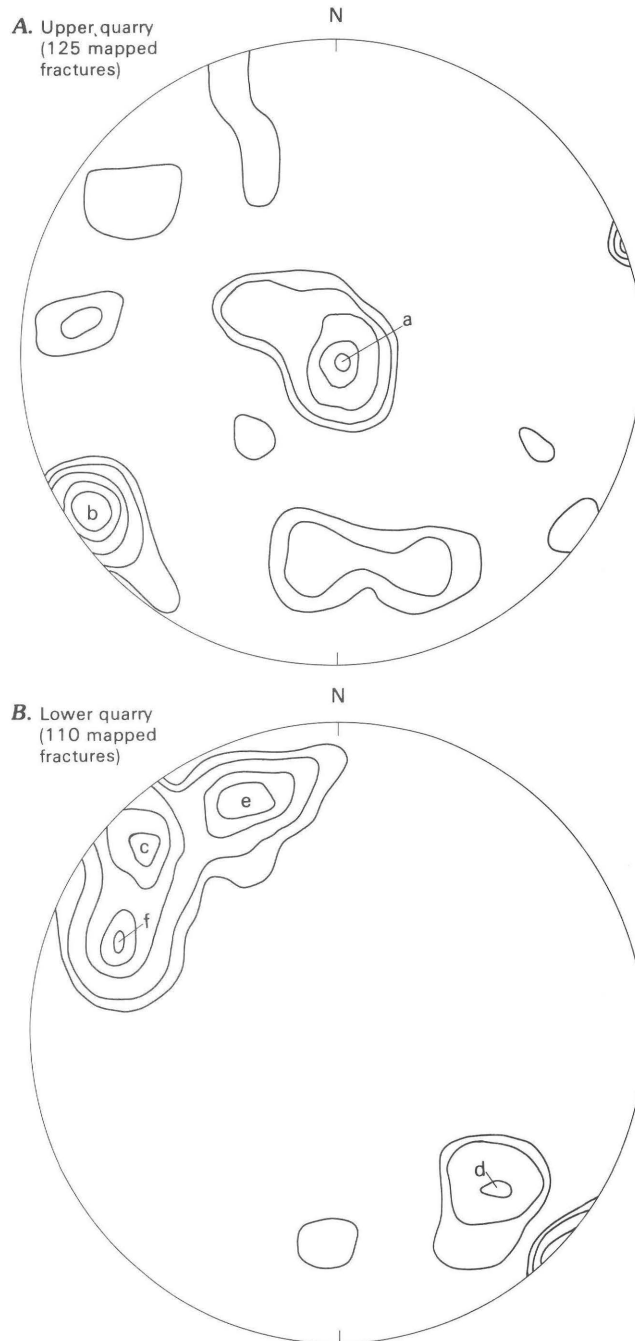


Figure 5. Equal-area diagrams (lower hemisphere) of poles to natural fractures mapped in the lower and upper quarry areas at Barre, Vt. Contours are at 2, 4, 8, 12, and 16 percent per 1 percent area. Orientation of major fracture sets shown by a-f: a is concentration of sheeting fractures; b, northwest fractures; c, d, e, and f are strongly developed northeast-trending conjugate fracture sets.

cluded that the dikes are primary features and therefore the fractures must have originated during or shortly after the forceful emplacement of the pluton. Continued uplift after the pluton solidified caused intense fracturing along and adjacent to the southern interior contact zones. The



Figure 6. Tendency of sheeting fractures developed in upper quarry area to terminate at boundaries of older fractures. Widely spaced horizontal parallel lines toward bottom of photograph are boundaries of old quarry lift planes. View is to the west.

northeast-trending fracture sets c and d (fig. 5B) with high-angle northwest, southeast dips imply a conjugate set, whose major principal stresses, σ_1 and σ_3 , at the time of fracturing were respectively vertical and to the southeast-northwest. Two more fracture sets, e and f (fig. 5B), striking respectively east-northeast and north-northeast with steep northwesterly dips, imply a possible second conjugate set of fractures. At the time of fracture, the major principal stresses, σ_1 and σ_3 , were nearly horizontal, bearing to the northeast and southeast, respectively, and σ_2 was nearly vertical. In either case the minimum principal stress (σ_3) was nearly horizontal, had a bearing southeast-northwest and may have coincided with regional tectonic relaxation subsequent to the Acadian orogeny.

Modal Composition and Petrofabrics

The composition of the Barre Granite has been statistically determined by Chayes (1952) to be very uniform, at least in five of the presently active quarries. Murthy (1957) checked Chayes' results, and found no significant differences. The results indicated that the granite contains about 26 percent quartz, 35 percent plagioclase, 19 percent potassium feldspar, 18 percent mica (both biotite and muscovite), and less than 2 percent accessory minerals.

Petrofabric analyses have been performed by Willard and McWilliams (1969), Thill and others (1973), and Engelder and others (1977). These investigators report strong preferred orientations of open and healed micro-

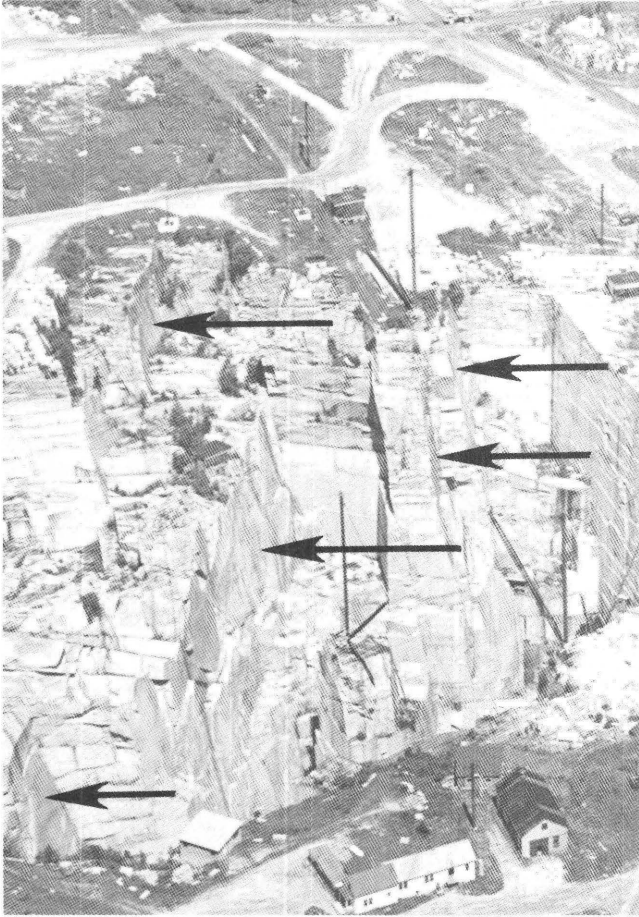


Figure 7. Very extensive but widely spaced northwest-trending fractures (arrows) found in the upper quarry area. View is to the northwest.

fractures nearly parallel to the rift plane. Thill's data show a second strong set of microfractures, parallel to the grain plane. These planes are respectively oriented vertical, striking to the northeast, and horizontal. The first two reports infer that a great number of the microfractures occur in the quartz grains. In addition, the Thill investigation reveals that there is little preferred orientation of the quartz, plagioclase, and mica grains but that there is a suggestion of orientation of twins within microcline grains in the rift plane. My petrographic examination of samples taken from the Wetmore and Morse quarry shows a similar strong orientation of two sets of microfractures (fig. 10), both open and healed, subparallel to the rift (N. 40° E., vertical) and lift planes (horizontal). The healed microfractures are seen here as bubble planes, according to an interpretation by Simmons and Richter (1976). This is supported by Shelton and Orville (1980), who formed synthetic fluid inclusions in fractured natural quartz by annealing samples at 600°C and 2 Kbar pressure in the

presence of water. Most of the microfractures are within the quartz grains and end abruptly at the quartz boundaries (fig. 10). In addition, strong undulatory extinction and subgrain development are associated with deformation of quartz grains, and according to Tullis and Yund (1977) these effects can occur at strain rates of 10^{-6} sec^{-1} within confining stress fields greater than 150 MPa at temperatures above 300°C. J. Tullis (written commun., 1979) also has examined some Barre Granite thin sections and states, "Judging from my experience with experimentally and naturally deformed quartzites, I would estimate that the microstructures shown by the quartz grains in this granite were produced at a temperature of close to 300°C (for a standard, slow natural strain rate of about $10^{-14}/\text{s}$)."

The petrographic evidence thus supports the idea that since the solidification of the magma, the granite has been subjected to temperatures greater than 300°C and burial depths greater than 7 km. The annealed microfractures also indicate strong dislocation activity occurring after an initial brittle deformation period. This suggests a reheating of the rock mass to over 300°C and the possibility of a superposed thermal event as mentioned by Zartman and others (1970) and Naylor (1971).

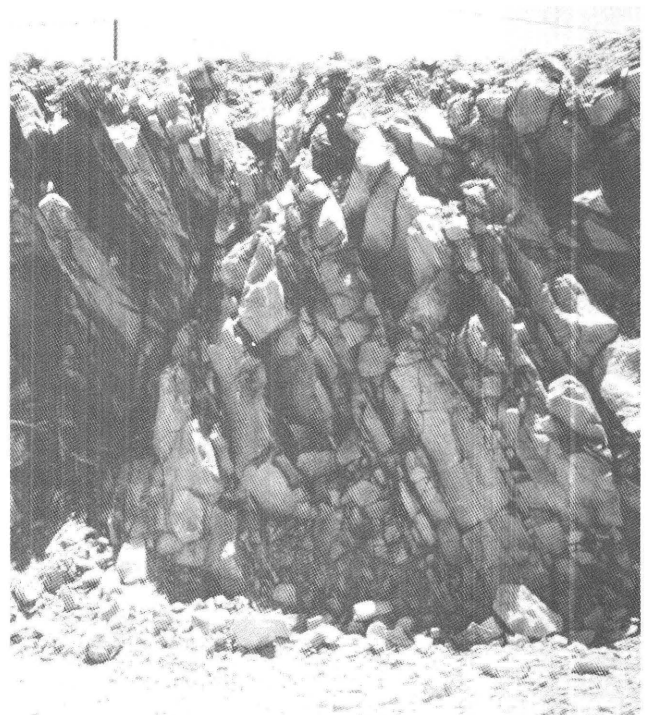


Figure 8. Well-developed northeast-trending shear zones found adjacent to granitic-metamorphic boundaries in the interior portion of the pluton, lower quarry area.



Figure 9. Well-developed northeast-trending fracture and shear zones seen in lower half of picture (arrows) terminate abruptly at massive unfractured granite of upper quarry area.

Site Selection

The site for our experiment in the Wetmore and Morse Quarry near Barre was selected on the basis of the following criteria:

1. The rock type present at the quarry. The Barre Granite is a very uniform hard rock with no obvious structural anisotropies other than fractures and microcrack fabric which have been extensively studied and documented. On the rock chosen for quarrying, two very fine sheeting fractures were discernable and easily mapped.

2. The geometry of the quarry and the $10 \times 10 \times 5.7$ -m block to be quarried, although not ideal, that was amenable to an elastic numerical analyses.

3. Previous observations of quarry deformations and failures that indicated deformations in response to quarrying of the chosen block would be easily measurable.

4. The many laboratory studies of the physical and mechanical properties of the Barre Granite that have been conducted.

5. The operator's plan for quarrying that allowed sufficient time and operating room to adequately investigate the prequarry and postquarry conditions of the $10 \times 10 \times 5.7$ -m block.

Deformation, Stress, and Temperature Measurements

Prequarrying measurements of the stress and strain fields in the $10 \times 10 \times 5.7$ -m granite block and surrounding rocks were made for a period of 15 months prior to quarrying of the block. The block was quarried by burn-cutting side channels with oxygen-kerosene torches and then splitting on the bottom horizontal plane with dynamite charges. After the block was quarried, it was left in place and postquarry measurements were made to determine the response of the block and adjacent rocks to removal.

Various deformation and temperature measurements were made on external surfaces and within the block and

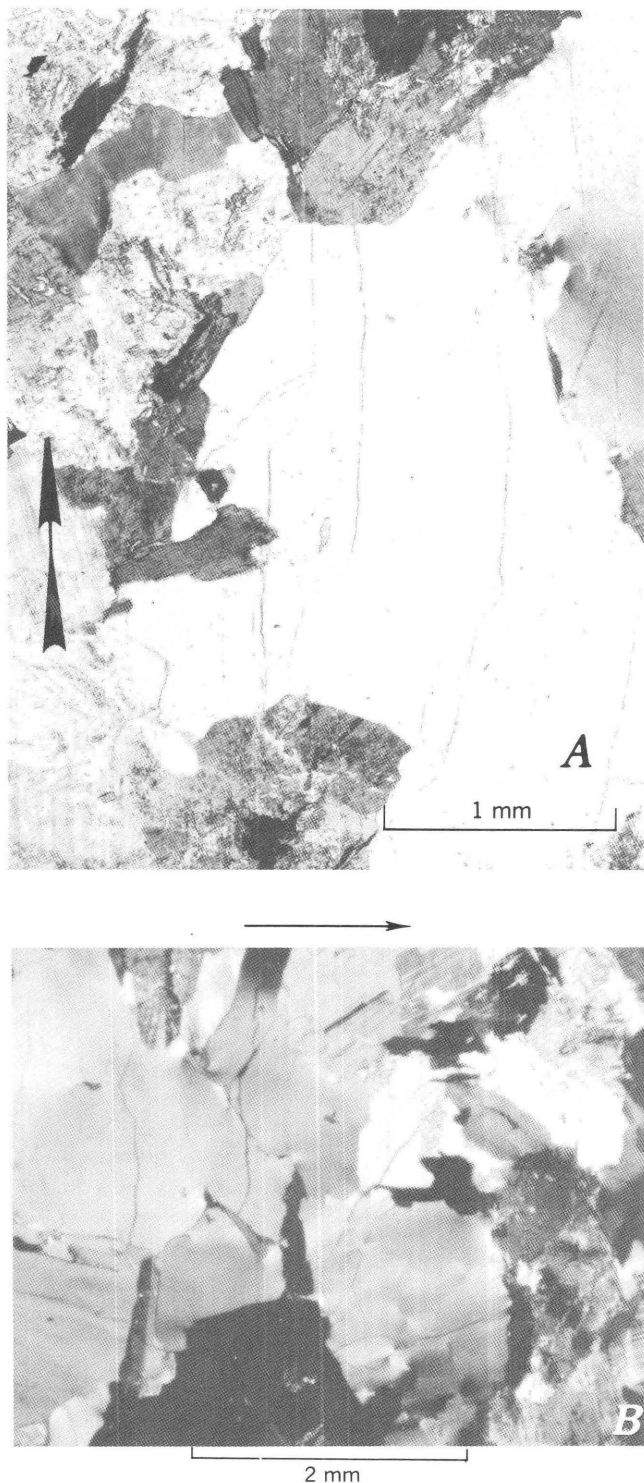


Figure 10. Examples of open and healed microcracks in quartz crystals, Barre Granite. Healed microcracks are seen as bubble planes. *A*, Plane of view is horizontal and direction (arrow) is N. 40° E. *B*, Plane of view is vertical and direction (arrow) is N. 50° W.

adjacent rocks during the field investigations, and on cores removed from the block before and after quarrying.

Type of Measurement and Locations

Rock-temperature measurements were monitored periodically with resistance type thermometers, in vertical holes drilled in the granite block and auxiliary holes just northwest of the block. The USGS three-dimensional probe installations (figs. 11, 12) in the block provided rock-temperature data for each installation.

Stress determinations within the granite were made using the overcoring techniques in vertical and horizontal core holes to depths of 8 m. The U.S. Bureau of Mines (USBM) and USGS measuring devices were used at equivalent depths.

An attempt was made to select several rock-stress measurement techniques in order to obtain independent data checks. Methods chosen were the commonly used overcoring and hydrofracturing techniques. The overcoring technique basically depends on measuring relief displacements that occur in the rock as it is cored and converting these to rock-stress values through measured elastic-rock constants. The hydrofracturing technique essentially depends on measuring fluid pressures required to balance rock pressures as fluids are injected into fractures.

For the overcoring procedure, three types of instrumentation were chosen: (1) the USBM three-axis borehole deformation gage (Hooker and Bickel, 1974), (2) the USGS three-dimensional borehole probe (Lee and others, 1976), and (3) metal-foil resistance strain gages (Swolfs, 1976).

The USBM gage was chosen because of its extensive successful use for measurements of this kind. The instrument is well designed and rugged, and can be used repeatedly. It was designed upon a sound theoretical basis for use in interpreting stresses in an elastic media. The instrument is a "soft modulus" device, meaning that it measures displacements, while offering little or no resistance to rock deformation. The disadvantage of using this device is that for any single measurement it can only be used to determine stresses in a single plane.

The USGS probe was chosen because it can be used to determine the 3-dimensional stress condition at the measurement location. Also, the instrument is a borehole inclusion, much stiffer than the USBM gage, and primarily monitors deformations and temperature changes. The theoretical basis for the gage is more complex than that of the USBM gage and also requires that the response of the rock be elastic. The instrument, although less expensive than the USBM gage, can only be used once.

Strain gages were chosen for very near surface measurements because they are the least expensive and can be easily applied to accessible rock surfaces. The theory used for stress interpretation is simple and requires that the monitored strains be those of the elastic response of the rock. Stresses can only be determined for the plane on which the gages are mounted.

A disadvantage of all three gages is that they cannot differentiate strains of thermal origin from those of stress changes. Compensation for or interpretation of thermal strains is required in each case. The first two instruments were installed in boreholes at various depths (figs. 11, 12) and overcored, whereas the strain gages were installed on prepared rock surfaces on the block prior to overcoring.

All of the data obtained from the overcore measurements are reported herein as stresses, using the assumption that the rock response during the overcore measurement was elastic. The data show evidence that the response was not entirely elastic and that the data perhaps more properly should be presented as displacement or strains. However, as there is doubt, and because the data are more simply reduced to stresses by the existing programs for each instrument, the data are left in terms of stresses and the arguments for elastic versus inelastic response will be presented in the discussion. The reader, therefore, is cautioned to view the stress data critically and to consider that the expression of these data may be more appropriate in terms of strain rather than stress. The principal directions of strain and the ratio of principal strain magnitudes would remain the same as for the stress values because the stresses have been calculated using an average elastic modulus and Poisson's ratio in all directions.

In addition, hydrofracturing tests were used to measure stresses at depths of 3.5 and 5.5 m in the block (fig. 12), but are not discussed further because the data were incomplete (Nichols, 1980).

To determine surface displacements, five displacement nets were established: two on the top surface, two on a vertical face of the block to be quarried, and one on a horizontal surface adjacent to the top of the block (fig. 13). The nets were each composed of three arms and covered most of the exposed surface of the quarried block. Each arm had measuring points at both ends that consisted of steel bolts that were mechanically wedged into drill holes. The bolts on nets 1 and 2 were spaced 6.05 m apart; on net 3, 1.89 m apart; on net 2E, 1.52 m apart; and on net 4, 4.15 m apart. The angles between arms were 60° on nets 1, 3, and 4; 45° and 90° on net 2. The nets were measured periodically with precision steel tapes that were calibrated for temperature change.

Additional strain and displacement measurements were made on cores that were removed from the large block both before and after quarrying. Strain gages were applied to external surfaces of solid cores and overcore annuli several hours after coring to continue monitoring strain relief with time. Continued measurements were made also across the central boreholes within overcore annuli. These latter measurements were made with the USBM borehole deformation gage.

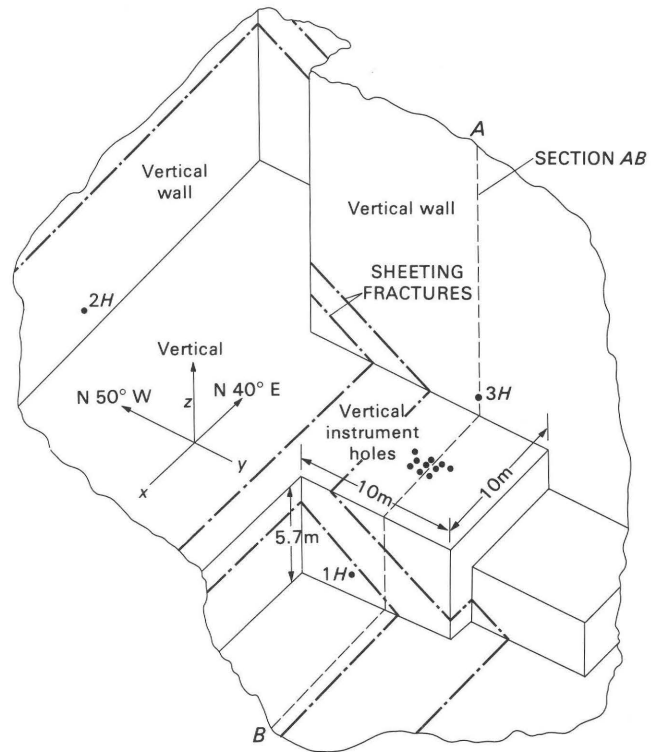


Figure 11. Perspective view of 10×10×5.7-m block of Barre Granite and adjacent quarry area, Wetmore and Morse quarry, Barre, Vt., showing locations of boreholes and sheeting fractures. The coordinate system (x , y , z) and the cross section (AB) were used in the finite-element calculation of gravity stresses. Horizontal instrument holes are designated by 1H, 2H, and 3H. The group of vertical instrument holes is shown in detail on Figure 12.

Results of Temperature Measurements

Figure 14 shows the average daily temperatures measured in the auxiliary holes at depths of 1.52, 2.74, 4.27, and 7.01 m during the periods of field investigation in July, October, and November 1975, and October and November 1976. In addition, the rock temperatures at all of the USGS 3-D probe installations to the time of overcoring are shown. Two of these probes were used to monitor temperature changes over a year's time at depths of 4.58 and 4.61 m in holes 1 and 1a on the block (fig. 12). The maximum spread of measured temperatures during the periods of field investigation was 2.78°C for all measurements except those at 1.5 m, but generally was much less than this, whereas at 1.5 m depth the temperature spread was much larger at 11.1°C. The 1.5 m temperatures ranged from 6.7°C warmer than temperatures below 3 m during the July 1975 investigations to 3.9°C cooler during the November 1976 investigations. The temperature variations on both USGS probes at the 4.6 m depth showed nearly identical responses with a maximum seasonal variation of 5.8°C.

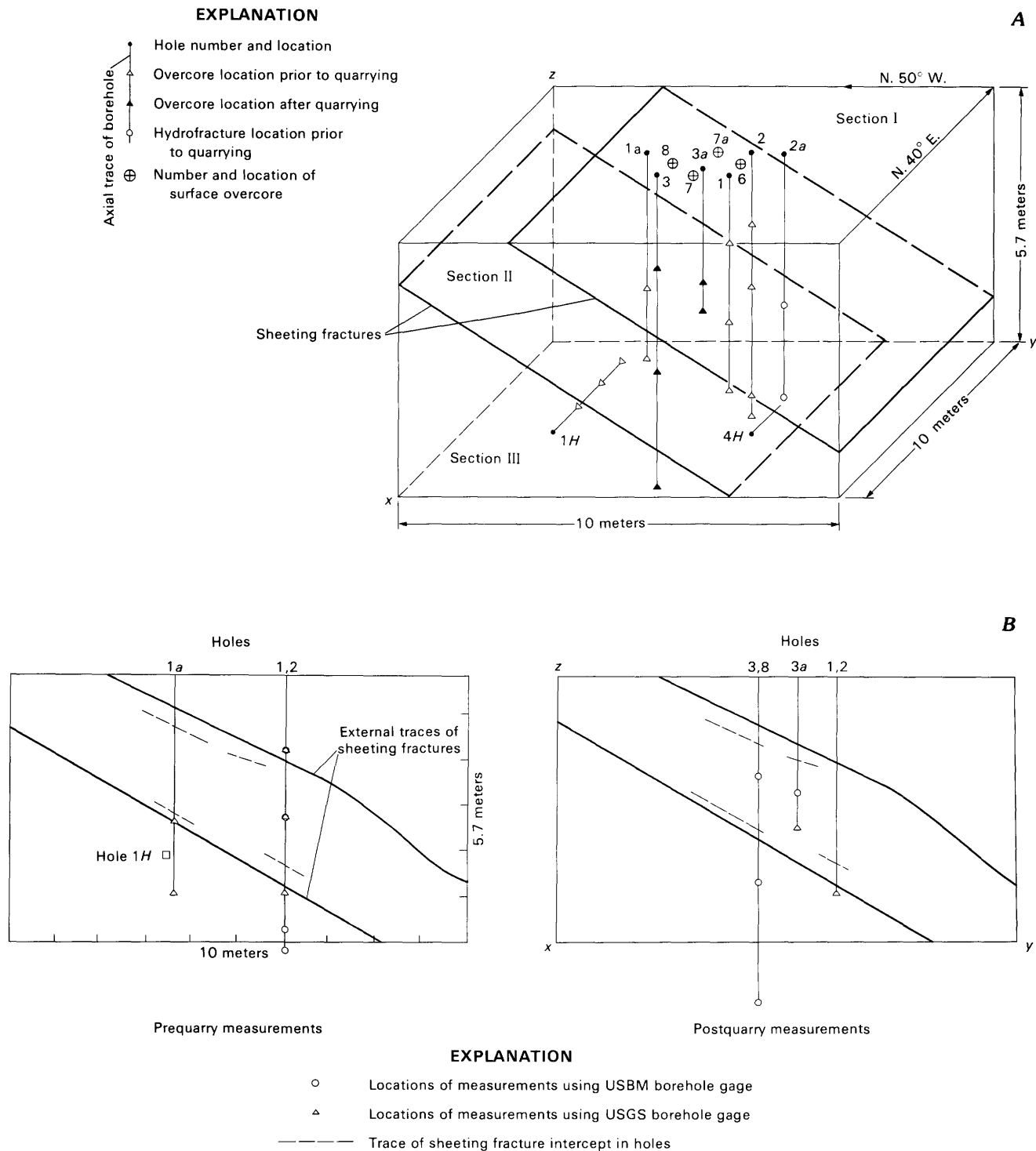


Figure 12. A, Isometric view of the 10×10×5.7-m block of Barre Granite showing borehole locations, overcore and hydrofracture locations, sheeting fractures, and coordinate axes x , y , and z , Wetmore and Morse quarry, Barre, Vt. Sections I, II, and III are separated by sheeting fractures. B, Section views of the same block showing locations of prequarry and postquarry overcoring stress measurements. Viewed normal to x axis. Dashed lines indicate location of sheeting planes in boreholes.

Because there were insufficient data on the thermal rock properties and thermal gradients within the block at the time of investigations, it is impossible to determine

the induced thermal stresses. The block in its unquarried position is essentially unbounded on the top and one side, thus not perfectly confined. However, based on thermal

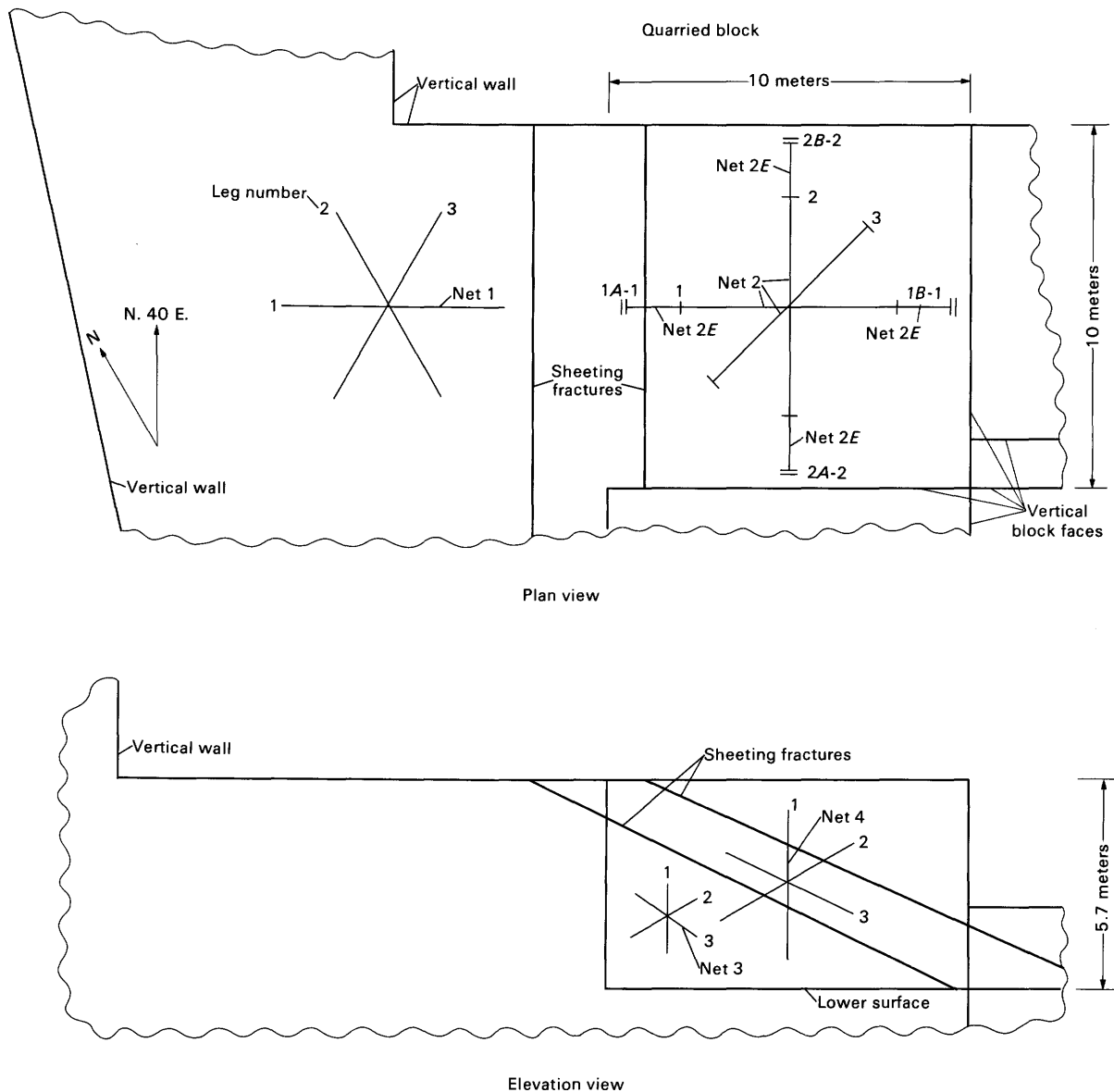


Figure 13. Locations of displacement nets 1, 2, 2E, 3, and 4, Wetmore and Morse quarry. Nets 1, 2, and 2E are on the top horizontal surface, where net 2E is an extension of legs 1 and 2 on net 2, and nets 3 and 4 are on the existing side vertical surface. Nets 2, 2E, 3, and 4 are on the unquarried 10×10×5.7-m block of Barre Granite.

stress data, Hooker and Duvall (1971) determined a thermal stress of approximately 0.305 MPa per °C for the Mount Airy Granite of North Carolina, assumed to be an elastic half space. Because the elastic constants of the Mount Airy Granite are very similar to those of the Barre Granite, this figure may be reasonable for thermal stresses at Barre. Therefore, thermal stresses, based on the temperature differences measured (0.85 MPa for 2.78°C difference), appear to be small enough to be neglected for the scope of this paper.

Prequarrying Stresses

Prequarry stress data and sign convention are given in table 1. The magnitudes and orientations of the maximum, intermediate, and minimum principal stresses σ_1 , σ_2 , and σ_3 and the maximum and minimum secondary principal stresses P and Q in the horizontal and designated vertical planes are shown according to their borehole location and depth of overburden. Stresses obtained by over-coring the USBM borehole gage were determined using

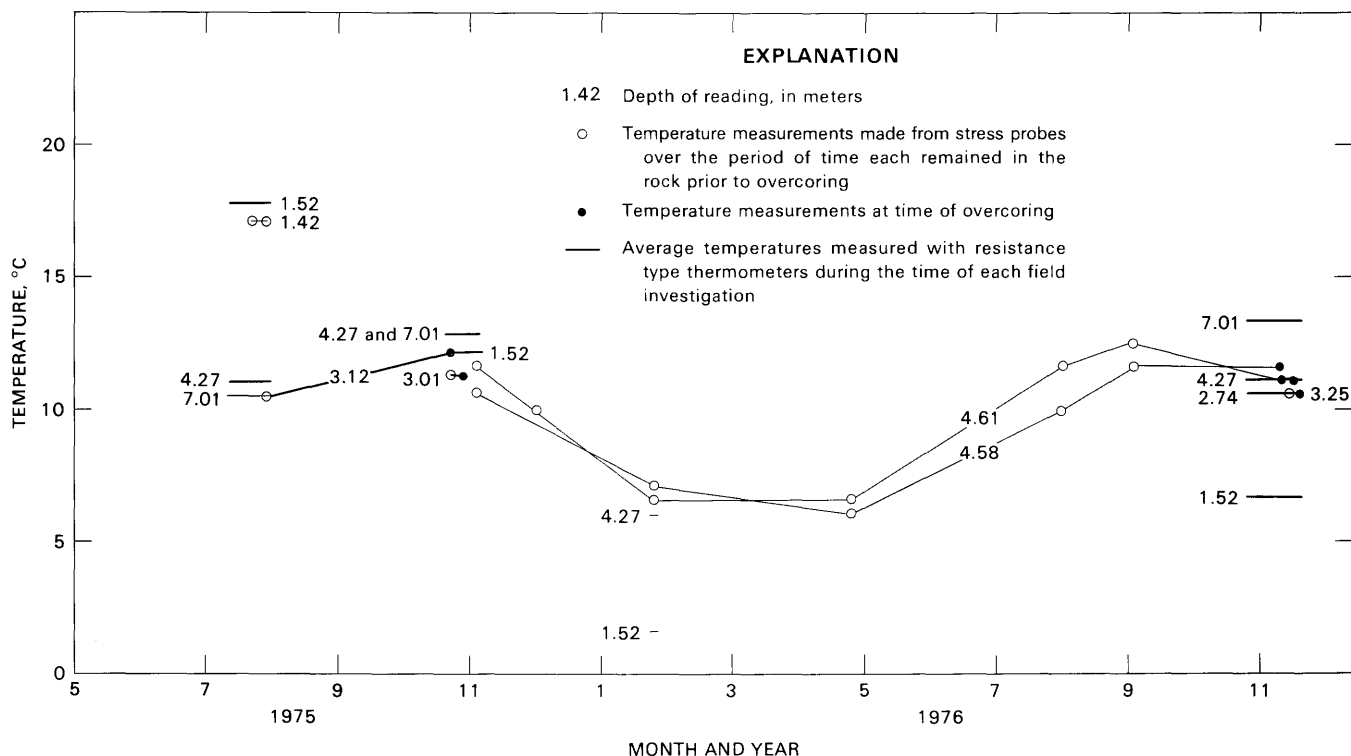


Figure 14. Measured temperature versus time in 10×10×5.7-m block and adjacent rock.

plane-strain analyses and lie in planes normal to borehole axes. For comparison, stresses determined by overcoring the USGS 3-D borehole probe were rotated into planes normal to borehole axes.

Overcore Measurements

The measurements made in the block were located in sections I, II, or III bounded by sheeting fractures (fig. 12A). These were made in vertical holes 1, 1a, 2, 6, 7, 7a, 8, and horizontal hole 1H. Therefore, all of the stress determinations made with the USBM gage except those made for hole 1H were in the horizontal plane. In that the top of the block was more fractured than the lower portions, the measurement locations near the top were closer to fracture surfaces. Effects of fracture proximity on stress distribution within sections I, II, and III can be seen on figure 15, which shows a plot of the maximum secondary principal stress magnitudes (P) versus the approximate distance of the stress measurement location from known fractures. Also, figure 15 shows a lower hemisphere plot of the stress orientations for these measurements. The distance of the measurement from a fracture appears to be a significant factor in determining the stress magnitude, much more so than the depth of measurement. The principal stress orientations on the other hand seem to be more a function of the section

location. The measurements made at the greatest distances from fractures have the greatest stress magnitudes apparently independent of the section location, whereas the stress orientations in sections I and II, independent of the proximity to fractures, are very similar and those in section III are consistently rotated more than 90° clockwise.

The directions of minimum secondary principal stresses (Q) determined from the surface measurements are from N. 40° E. to N. 48° E., demonstrating that near or on the surface, Q is parallel to the rift plane (N. 40° E.). The findings of Swolfs (1976) and of Engelder and others (1977), who both made strain relaxation measurements on surface rocks of the Barre quarries, also led them to conclude that minimum strains are parallel and maximum strains are normal to the rift plane. They inferred that the mechanism of strain relaxation in the Barre Granite was the opening of microcracks in the rift plane. This appears to be true only near the surface of section I.

Horizontal hole 1H in section III is under 3.85 m of overburden. The stress components measured at three locations in this hole are in vertical planes that strike N. 50° W. The magnitude and plunge of P and Q for each measurement are very consistent, and P agrees well with the measurement made in horizontal planes, the maximum being 8.43 MPa, plunging 25° to the southeast. This value, like the other values of P in section III, does not appear to be affected by the sheeting fractures.

Table 1. Determinations of stresses (MPa) made on Barre Granite adjacent to and within the 10×10×5.7-m block prior to and after quarrying, Wetmore and Morse quarry, Vermont

[σ_1 , s_2 , and σ_3 , are principal stresses. P and Q are secondary principal stresses that are determined in a horizontal plane and a vertical plane with the strike the same as the bearing. Positive stresses are compressional and negative stresses are tensile. Maximum principal stresses P and σ_1 are the most compressive. Leaders (--) indicate no data]

Hole No.	Over-burden depth (m)	Distance ¹ (m)	Section ²	P	Q	Attitude of P (degrees)		σ_1	σ_2	σ_3	Attitudes, in degrees					
						Bearing	Plunge				σ_1		σ_2		σ_3	
											Bearing	Plunge	Bearing	Plunge	Bearing	Plunge
Prequarrying measurements																
Overcore, USGS 3-D probe																
1	1.42	1.42	I	-0.35	-0.92	N. 11 W.	0	0.09	-0.36	-0.95	N. 68 W.	79	S. 9 E.	6	N. 80 E.	9
1	3.12	3.12	II	6.34	.31	N. 3 W.	0	9.63	3.07	.28	N. 0 W.	45	S. 9 E.	45	S. 85 W.	5
1a	3.01	3.01	III-II	1.50	.16	N. 15 W.	0	1.60	.21	-.73	S. 13 E.	12	S. 80 W.	12	N. 34 E.	73
1a	4.58	4.58	III	6.29	3.58	N. 88 W.	0	6.29	4.89	2.16	S. 87 E.	2	S. 4 W.	44	N. 1 E.	46
Block lift, USGS 3-D probe ³																
1	4.61	4.61	III	6.44	3.74	N. 86 E.	0	6.80	4.41	3.28	N. 82 E.	21	N. 31 W.	45	S. 9 W.	37
Overcore, USBM 3-axis probe																
2	1.53	1.53	I	.57	.29	N. 22 W.	0	----	----	----	-----	--	-----	--	-----	--
2	3.05	3.05	II	5.70	1.27	N. 26 W.	0	----	----	----	-----	--	-----	--	-----	--
2	5.34	5.34	III	8.78	4.63	N. 88 W.	0	----	----	----	-----	--	-----	--	-----	--
2	5.80	5.80	III	9.58	5.28	N. 89 W.	0	----	----	----	-----	--	-----	--	-----	--
1H	3.87	1.64	III	7.22	.97	S. 50 E.	20	----	----	----	-----	--	-----	--	-----	--
1H	3.84	3.28	III	8.43	1.98	S. 50 E.	24	----	----	----	-----	--	-----	--	-----	--
1H	3.81	4.92	III	8.17	1.66	S. 50 E.	25	----	----	----	-----	--	-----	--	-----	--
2H	67	1.64	-----	17.99	2.26	N. 40 E.	60	----	----	----	-----	--	-----	--	-----	--
2H	67	3.28	-----	12.4	6.13	N. 40 E.	57	----	----	----	-----	--	-----	--	-----	--
2H	67	4.92	-----	6.21	1.95	N. 40 E.	10	----	----	----	-----	--	-----	--	-----	--
Overcore, metal-foil strain gage																
6	-----	0	I	8.28	2.07	N. 42 W.	0	----	----	----	-----	--	-----	--	-----	--
7	-----	0	I	2.32	.58	N. 46 W.	0	----	----	----	-----	--	-----	--	-----	--
8	-----	0	I	0	0	-----	--	----	----	----	-----	--	-----	--	-----	--
7a	-----	0	I	3.89	1.90	N. 50 W.	0	----	----	----	-----	--	-----	--	-----	--
3H	40	0	-----	9.1	6.62	N. 50 W.	6	----	----	----	-----	--	-----	--	-----	--
Postquarrying measurements																
Overcore, USGS 3-D probe																
1	4.61	4.61	III	-.99	-2.32	N. 28 E.	0	0.9	-1.04	-2.35	N. 51 E.	79	S. 26 W.	10	N. 63 W.	4
3a	3.25	3.25	II	.11	-.27	N. 34 E.	0	.82	.11	-.45	N. 60 W.	68	N. 32 E.	1	S. 57 E.	22
Overcore, USBM 3-axis probe																
3	2.10	2.10	II	.28	-.18	N. 45 W.	0	----	----	----	-----	--	-----	--	-----	--
3	4.42	4.42	III	-.09	-.65	N. 87 W.	0	----	----	----	-----	--	-----	--	-----	--
3a	2.53	2.53	II	.42	-.44	N. 49 W.	0	----	----	----	-----	--	-----	--	-----	--
3	7.02	7.02	(⁴)	9.63	4.92	N. 82 W.	0	----	----	----	-----	--	-----	--	-----	--

¹ Distance of measurement from surface.² See figure 12A.³ Stresses were determined by changes caused by quarrying of block.⁴ Measured in unquarried rock below section III after the overlying block was quarried.

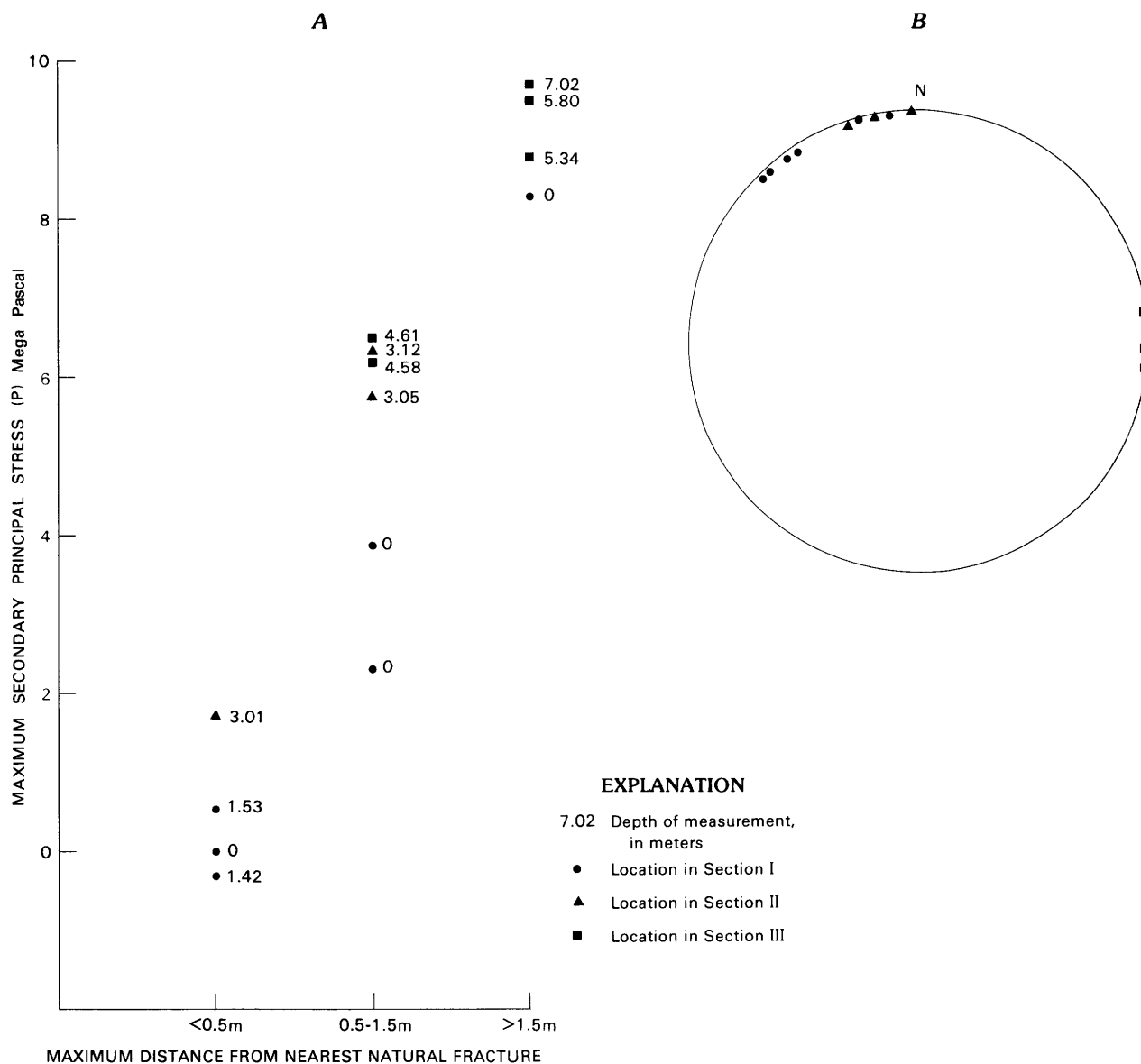


Figure 15. A, Plot of maximum secondary principal stress magnitudes (P) measured on the block versus maximum distance of stress measurement location from known fractures. B, Equal area diagram (lower hemisphere) showing orientations of the secondary maximum principal stresses (P).

The orientations of the three-dimensional principal stresses (σ_1 , σ_2 , σ_3) are plotted on a Schmidt equal area net on figure 16. Figure 16A shows σ_1 , σ_2 , and σ_3 for the stresses remaining in the block after relief caused by natural fractures or by quarrying the block. The stresses measured in sections I, II, and III in hole 1 at 1.42 m (1-1.42) and in hole 1a at 3.01 m (1a-3.01) are prequarry stresses that remain after relief by the sheeting fractures. Also shown for comparison are the postquarry stress orientations determined in sections II and III in hole 1 at 4.61 m (1-4.61) and hole 3a at 3.25 m (3a-3.25) that remain after relief by the quarrying operation. The directions of the free block sides, N. 40° E. and N. 50° W., and the orientation of the sheeting fractures are also

shown. The fracture-relieved stress orientations at 1-1.42 and 1a-3.01 are subparallel and subperpendicular to the fracture orientation and appear to be influenced by the geometry of fracture development, and possibly by the nonrelieved principal stresses of block section III (at locations 1-3.12, 1-4.61, and 1a-4.58) seen on figure 16B, which bear in similar directions. The postquarry stress orientations, however, at 1-4.61 and 3a-3.25 (fig. 16A), as would be expected, are nearly parallel and perpendicular to the quarried block sides, and thus, seem to be controlled by the block geometry.

Other prequarrying stress measurements were made in horizontal boreholes 2H and 3H drilled into the vertical walls to the southwest and northwest of the large block

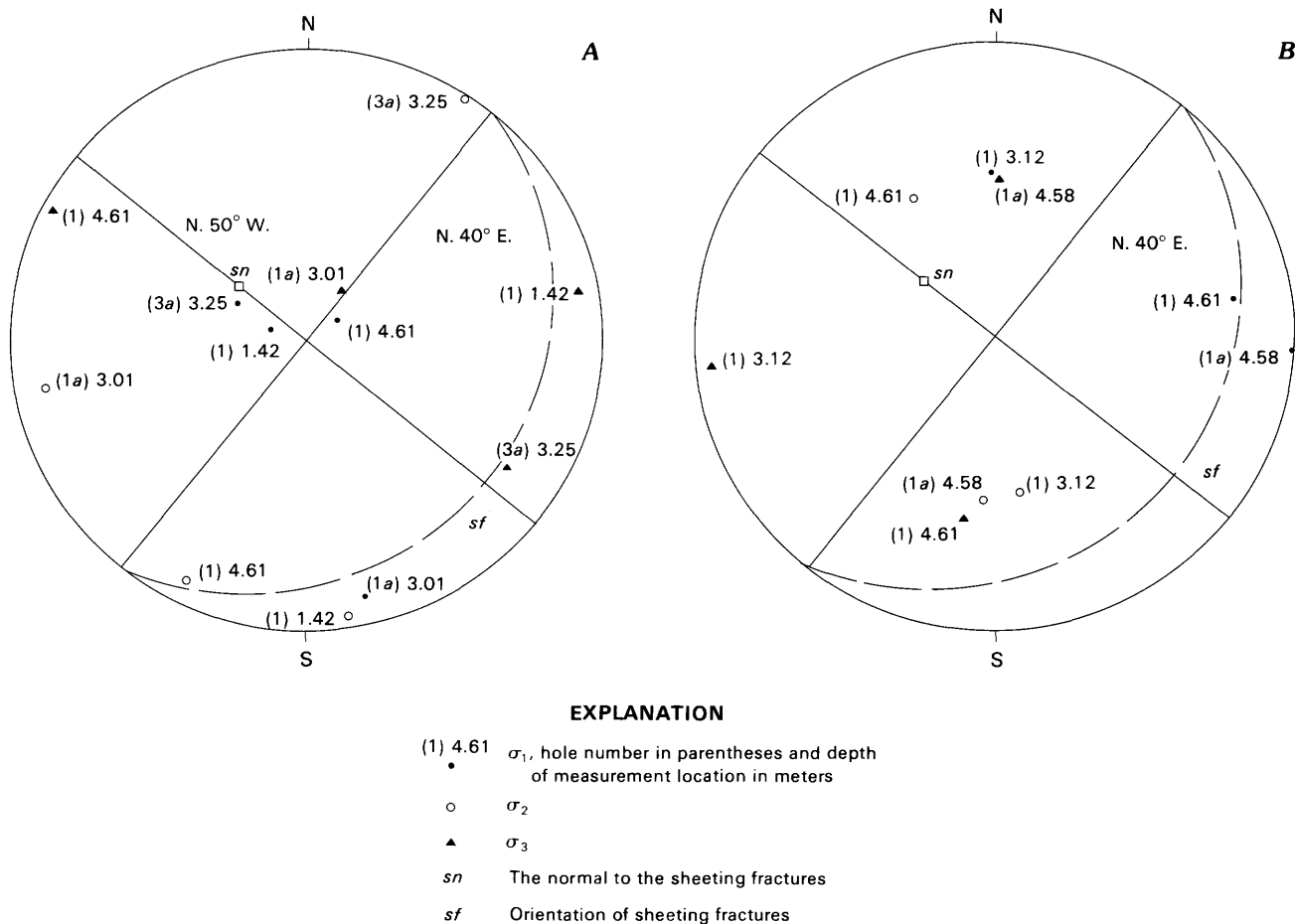


Figure 16. Equal area diagrams (lower hemisphere) showing orientations of principal stresses determined within 10×10×5.7-m block of Barre Granite. A, stress orientations measured at locations relieved either by quarrying of block or by natural fractures. B, stress orientations unrelieved, prior to quarrying of block.

(fig. 11). Hole 2H is under 67 m of overburden (fig. 2). The three stress determinations made in this hole at distances of 1.64, 3.28, and 4.92 m from the vertical wall (fig. 11) demonstrated horizontal stresses to be very similar to the unrelieved stresses measured in the same direction in the unquarried block (table 2). The vertical stresses (table 2), however, from the first two measurements were several times greater than the vertical stress in the block, whereas the vertical stress of the third measurement was slightly less than nearly all of the unrelieved vertical stresses determined in the block. The third measurement, although 4.92 m into the granite face, was less than 0.5 m from an iron-stained fracture dipping to the southeast at about 45°. The measurement location was in the footwall side of the fracture underlying at least 67 m of overburden. Hole 3H is under about 40 m of overburden. One stress determination was made at this location on the surface of the vertical wall that strikes N. 50° W. This was done by overcoring strain gages mounted on a prepared vertical surface (Swolfs, 1976), and the determined horizontal stress was slightly higher than those unrelieved horizontal stresses measured in the N. 50° W.

direction in the block. The vertical stress was more than double the vertical stress in the block but less than half of the vertical stress in hole 2H near the face of the other highwall.

From the prequarry stress measurements made in the vicinity of the block, several distinctive characteristics were revealed.

1. The determined stress magnitudes and orientations are strongly influenced by relief within 0.5 m of fractures and free surfaces. Stresses normal to planes parallel to these surfaces are the most severely affected.

2. The principal stress orientations away from fractures in the unquarried block appear to be related more to spatial locations and geometry than to fracture orientations. The near-surface stress orientations may be related to a microfabric feature, the rift plane, whereas for deeper measurements, this relation is not apparent and directions appear to be controlled by the section location.

3. The determined horizontal stress magnitudes do not appear to change much as a function of depth of overburden, whereas the vertical magnitudes increase considerably at depth.

Table 2. Measured and gravity stresses (MPa) in the x, y, and z directions in Barre Granite adjacent to and within the 10×10×5.7-m block prior to quarrying

[σ_x , σ_y , and σ_z are normal stresses in the N. 40° E., N. 50° W., and vertical directions. Measured and calculated gravity stresses are indicated by m and g. Positive stresses are compressional and negative stresses are tensile. Calculated stresses are based on a plane-strain finite-element calculation using the overburden load and Poisson's ratio of 0.25. Leaders (--) indicate no data]

Hole No.	Overburden depth (m)	σ_x		σ_y		σ_z	
		(m)	(g)	(m)	(g)	(m)	(g)
Overcore, USGS 3-D probe							
1	1.42	-0.69	0.27	-0.58	0.07	-0.06	0.10
1	3.12	3.05	.48	3.60	.13	6.33	.26
Block lift, USGS 3-D probe ¹							
1	4.61	5.05	.50	5.14	.19	4.33	.42
Overcore, USGS 3-D probe							
1a	3.01	.61	.48	1.05	.13	.59	.26
1a	4.58	5.25	.50	4.62	.19	3.47	.42
Overcore, USBM 3-axis probe							
2	1.53	.36	.27	.50	.07	-----	----
2	3.05	2.06	.48	4.91	.13	-----	----
2	5.34	6.14	.48	7.28	.23	-----	----
2	5.80	6.91	.45	7.95	.27	-----	----
1H	3.87	-----	----	6.49	.9	1.70	0.29
1H	3.84	-----	----	7.37	.13	3.05	0.28
1H	3.81	-----	----	7.01	.17	2.83	0.36
2H	67	6.19	.80	-----	----	14.06	2.80
2H	67	7.99	.70	-----	----	10.54	2.10
2H	67	6.08	.66	-----	----	2.08	1.90
Overcore, metal-foil strain gage							
6	0	2.19	0	8.16	0	-----	----
7	0	.58	0	2.32	0	-----	----
8	0	.00	0	0	0	-----	----
7a	0	1.90	0	3.89	0	-----	----
3H	40	-----	----	9.10	1.00	6.62	----

¹Stresses were determined by changes caused by quarrying of block.

Measured Prequarry Stresses Compared to Predicted Gravity Stresses

Table 2 shows normal stress components in the x, y, and z directions (fig. 11) calculated from prequarry measurements. These directions, respectively, N. 40° E., N. 50° W., and vertical, bound the unquarried rectangular block and lie within and normal to the section AB (fig. 11). Gravity stresses in the AB plane for the x, y, and z directions were determined by a plane-strain finite-element calculation (Nichols and others, 1977) using the assumption that the confinement in the y direction is sufficient to allow little or no strain. The closest free surface from plane AB in the y direction is the small vertical surface at the upper southeast side of the block. Its distance from the AB plane is sufficiently far that by St. Venant's principle it is assumed not to have a large effect

(Sokolnikoff, 1956) on the confinement of the unquarried block. The stresses are contoured on figure 17 and reported for each measurement site in table 2. The measured horizontal stresses in most cases are at least five times greater than the calculated horizontal gravity stresses. Most of the measured vertical stresses are from 5 to 20 times the calculated vertical gravity stresses. The measured horizontal stresses under 6m and 67 m of overburden are approximately the same, whereas the measured vertical stresses at 67 m are much greater than at 6 m and are at least five times the calculated vertical gravity stresses in most locations. There are a few measurements that do not conform to this trend, those at 1.42 m in borehole 1, 3.01 m in borehole 1a, and 4.98 in borehole 2H. These measurements are all very close to sheeting fractures which probably relieved much of the stress. The majority of measurements at this location therefore indicate that unless relieved by fracturing the horizontal stresses remain approximately the same to a depth of 67 m, whereas the vertical stresses increase with depth and have a 5:1 ratio to the calculated gravity stresses.

Thus, the prequarry state of stress in the block and surrounding rock mass, as determined by overcore measurements and assuming an elastic rock response, appears to be different from one caused by gravity loading alone. Both the measured horizontal and vertical stresses are much greater (by at least a factor of 5) than those predicted by the gravity model. The measured stresses also differ from the gravity model in that both the horizontal and vertical stress components of the gravity model increase with depth, whereas only the vertical component of the measured stresses appears to increase significantly with depth. Also, the measured vertical component increases with depth at a much greater rate than does the vertical gravity component.

Stress Changes and Surface Deformations Caused by Quarrying

Stress determinations made in the 10×10×5.7-m block after quarrying (table 1) were used to determine changes in the block caused by quarrying. The determined prequarry stress magnitudes seemed to be a function of distance away from natural fractures, and within 0.5 m of natural fractures these stresses were greatly relieved. Therefore, the relief that occurred within the block as a result of quarrying was a function of distance away from natural fractures. After quarrying, stress determinations in sections II and III of the block show the secondary principal stress magnitudes (P and Q in table 1) to be between 0.42 and -2.32 MPa with a mean value of $\frac{(P+Q)}{2}$ of -0.41 MPa. The mean maximum principal stress (P) after quarrying is -0.05 MPa; therefore, it appears that on relief, the net state of stress in the block is one of slight tension

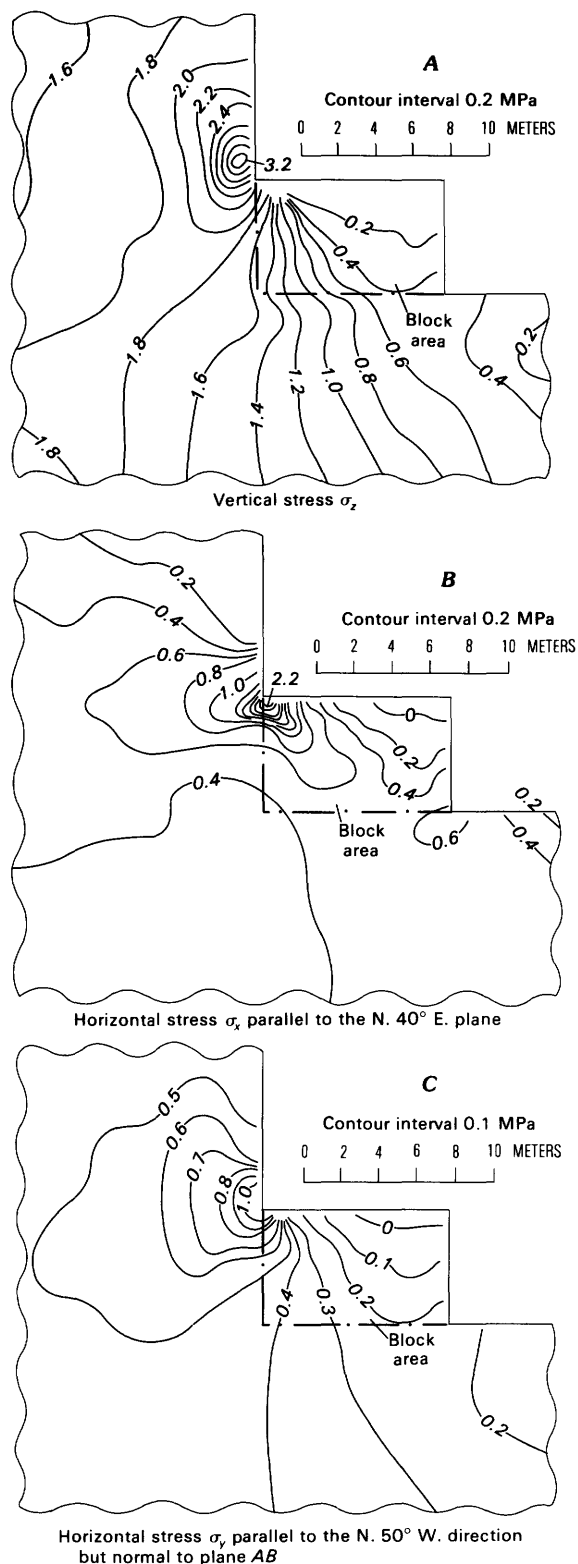


Figure 17. Gravity stresses determined by a plane-strain finite-element calculation in the vertical plane AB (fig. 11), striking N. 40° E., cutting the quarry wall and the unquarried block of Barre Granite, Wetmore and Morse quarry. For this calculation, Young's modulus was 31 GPa, Poisson's ratio was 0.25, and the density was taken to be 2.7 g/cm³.

possibly as a result of thermal stresses. By comparing the values of the prequarry and postquarry maximum principal stresses (P, table 1) in sections II and III, the stress reduction has been determined to be on the order of 1.6 to 9.6 MPa. If section I relieved in a similar manner, determined stress drops as large as 8.3 MPa are probable. Data from a USGS 3-D stress probe situated in section III (hole 1a, 4.58 m), during the final separation of the block on the lift plane, showed an initial maximum stress decrease of 6.5 MPa, which is consistent with stress measurements at this depth (table 1) before and after quarrying.

After the block was quarried, initial rapid surface deformations, measured on the surface nets, were followed by slower time-dependent deformation. The surface-displacement nets were measured just before and for 10 days after the block was quarried.

The changes on each leg could be measured to the nearest 25 μ m, which, over a gage length of approximately 6 m, is a strain of 4.2×10^{-6} . Considering that the stress release caused by quarrying may have been as large as 9.6 MPa, the resulting extensional strains are on the order of 350×10^{-6} . The displacement measurements, therefore, are considered to be sufficiently sensitive to monitor the displacements caused by stress release. Figure 18 shows the data for these readings on nets 1, 2, 2E, and 3. The displacements on nets 1 and 2 were converted to strains from which strain ellipses were calculated to determine principal strain directions. From the first-day strain ellipse determined for net 2, plane stress changes were determined which are also shown on figure 18. The 1-day interval is based on the assumption of a nearly linear elastic response.

Net 1, on the unquarried adjacent horizontal surface, showed mostly initial rapid contractions 1 day after quarrying, which were followed by slower and much larger contractions for 10 days. The lengths of legs 1, 2, and 3 were respectively 5.94, 5.94, and 5.85 m. After 1 day, legs 1 and 2 showed contractions of 559 and 356 μ m, respectively, and leg 3 showed expansion of 76 μ m. Contractions for the 10-day period were 2.03, 0.94, and 1.32 mm, respectively. The calculated strain ellipses show the maximum strain after the 1st day to be 110×10^{-6} bearing N. 20° W., and after the 10th day to be 354×10^{-6} bearing N. 70° W.

Nets 2 and 2E responded in overall expansion rather than contraction. The lengths of legs 1, 2, and 3 of net 2 were 5.85, 6.04, and 6.04 m, respectively. The expansions on these legs the 1st day after quarrying were respectively 0.25, 1.17, and 0.69 mm and the 10th day after quarrying were 0.53, 1.91, and 1.55 mm. The maximum calculated extensional strain for the 1st day was -193×10^{-6} bearing N. 37° E. which, if elastic, is equivalent to a maximum stress relief of 6.7 MPa in the same direction. For 10 days, the maximum strain was

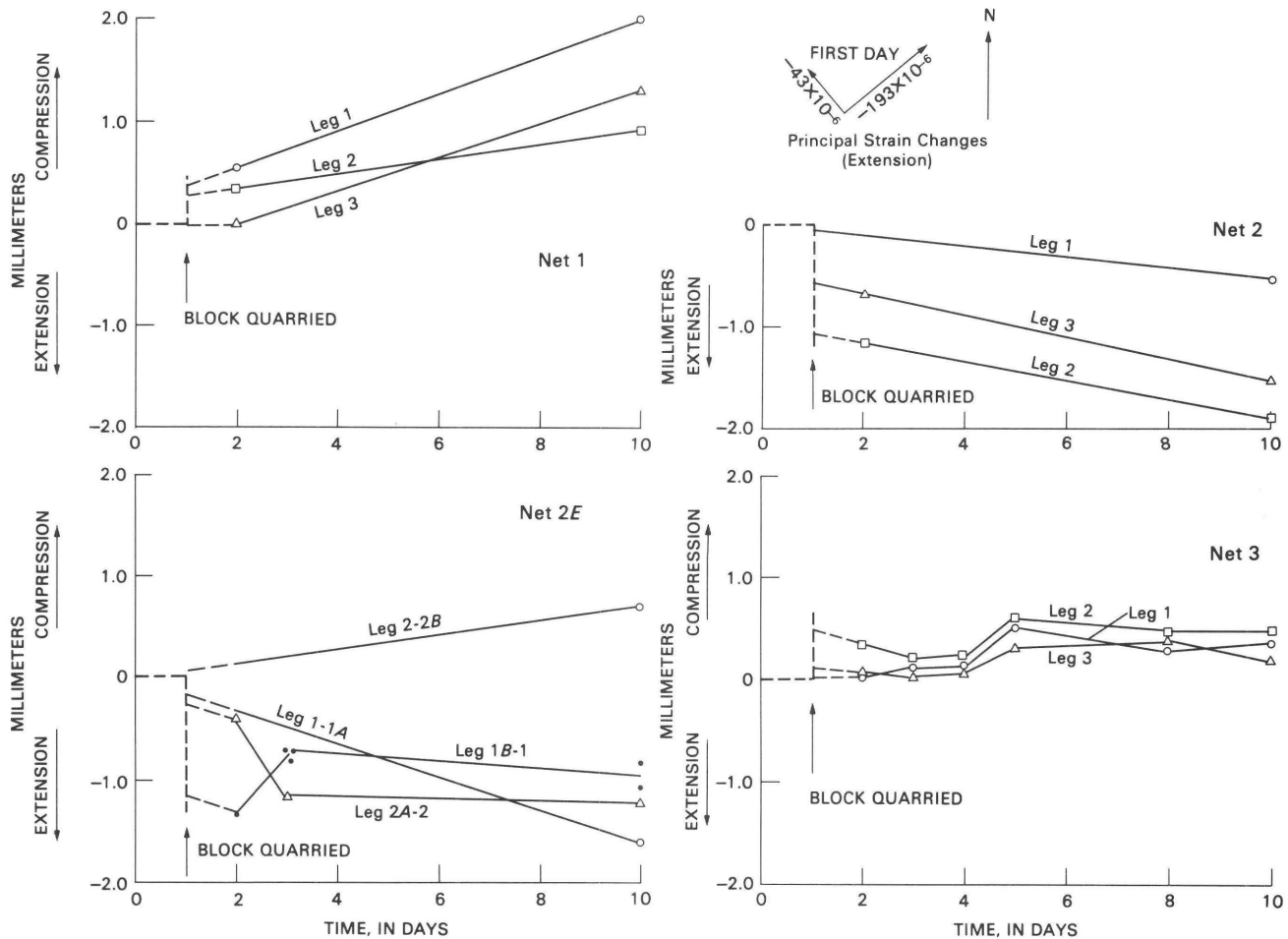


Figure 18. Graphs showing displacements versus time for nets 1, 2, 2E, and 3 after the 10×10×5.7-m block of Barre Granite was quarried. Principal strain changes for the initial first-day response for net 2 are shown.

-327×10^{-6} bearing N. 52° E. The initial expansions the 1st day after the block was quarried had about the same orientation and a little more than half the magnitude of those measured after 10 days.

Net 3, on the vertical southwest face of the quarried block, demonstrated initial compressive displacements after 1 day and subsequent comparable time-dependent displacements after 10 days.

Net 4 was located across both sheeting fractures. These fractures apparently sustained movement that made the deformation ellipse calculations of the net unrealistic; therefore, the calculations are not reported here.

Important points to note: (1) After quarrying, the 10×10×5.7-m block of granite appears to be almost totally stress relieved. The final average state of stress appears to be slightly in tension. (2) The stress reduction is a maximum of 9.6 MPa. (3) In most cases the time-dependent surface deformations were of the same sense and comparable in magnitude to the initial deformations. (4) The magnitudes of initial horizontal stress releases calculated for surface net 2 (fig. 19) are comparable to the stresses measured in the block before quarrying (table 1).

These magnitudes of released stresses on the surface are also comparable to the stress changes measured by stress instrumentation in the interior of the block (section II) during quarrying (table 1).

Time-Dependent Deformation of Cores

The cores retrieved from boreholes continued to deform with time, much in the same manner as the time-dependent deformations observed on a larger scale on the surface-deformation nets. In addition, 5.7-cm-diameter cores retrieved from instrument hole 5, drilled after the block was quarried, demonstrated considerable diskings (fig. 19). The diskings occurred in cores taken from depths as much as 2 m prior to removal from the core barrel. Cores further dissected in the laboratory also demonstrated additional release of time-dependent strains. Previous tests performed in the laboratory on a cube of Barre Granite (Nichols, 1976) demonstrated the same phenomenon.

Conceivably, extensional fractures, both natural sheeting fractures and quarry-induced fractures may occur as a result of inelastic unloading strains. Measured and

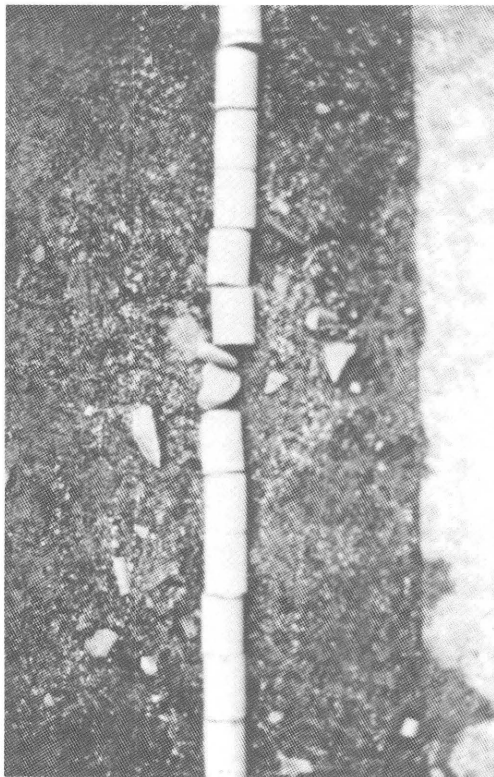


Figure 19. Disking (regularly spaced tensile failures) of 5.7-cm-diameter cores retrieved from hole 5 drilled after the 10×10×5.7-m block was quarried. Disking occurred in cores taken to a depth of 2 m in Wetmore and Morse quarry, Barre, Vt.

inferred strains of this nature are further discussed here as possible causes of failure.

Disking, described as extensional failure normal to core axes that occurs as a result of coring, has been interpreted to require large radial compressive stresses (Durelli and others, 1968) applied at the bottom of the rock cut surface (kerf). In the quarried granite block, however, there were no externally applied forces; therefore, the observed disking (fig. 19) must have resulted from extensional strains resulting from coring. At any rate, the fractures occurred after the rock was cored from the quarried block and were accompanied by time-dependent extensional axial strains sufficiently large to cause failure.

The overcore annuli extracted from the 10×10×5.7-m block during the overcoring process also continued to creep, as did the surface of the block. Within 6 hours after each overcore extraction, the annulus was removed and a second USBM deformation instrument, not being used for field operations, was placed in the central 3.8-cm-diameter borehole, and displacements were then monitored under conditions of small temperature variations and ambient humidity. Maximum and minimum displacements, U_1 and U_2 , that occurred with time in addition to those of the initial overcore are listed in table

3. These values were calculated using a 60° rosette analysis to determine displacement ellipses. The data show that the absolute value of the time-dependent displacements occurring as a result of cutting new rock surfaces within an intact rock mass can be as large as or larger than those of the initial displacements. Figure 20 shows the magnitudes of principal strain changes that were monitored by 45° strain-gage rosettes applied to the external core surfaces within 3–4 hours after each core was cut. The 90° gage elements were oriented to measure axial and circumferential strains. All of the external strains on the overcore annuli were extensional, whereas the internal borehole showed both extensional and shortening displacements.

Some of the core samples were returned to our constant-temperature and humidity laboratory in Denver for further monitoring and creep studies. Curve A on figure 21 shows the continuous creep behavior of a 5-cm core from the time of its removal in the field. Curves B and C show the plots of gages that were mounted on the same core, 200 and 530 hours after it was cored. The gages were read within 3 hours after installation and were periodically monitored in a constant-temperature and humidity room. Very little change was observed over a period of approximately 3 months. Superposed on the creep curve is a theoretical model of viscoelastic response derived by Savage (Nichols and Savage, 1976) for the Barre Granite, suggesting that the actual measured response may fit such a model.

Most core-drilling procedures carried out in crystalline rocks require the use of water to carry away cuttings

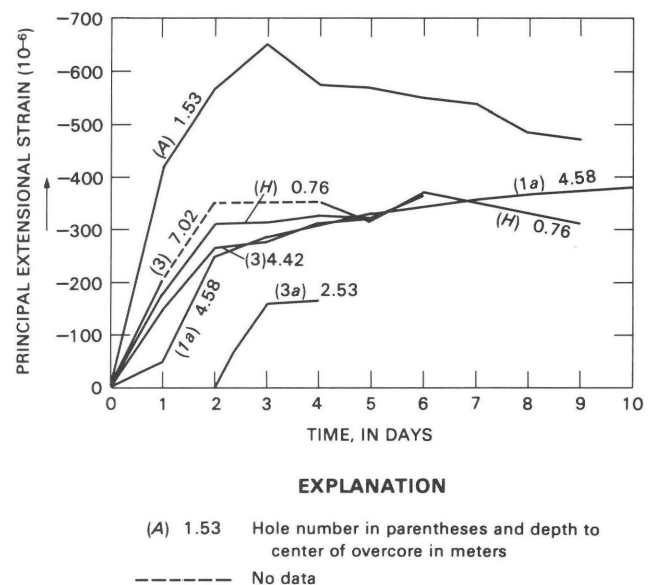


Figure 20. Extensional strains measured through time on exterior of overcore annuli after extraction from borehole. Overcore holes A and H were drilled in surfaces adjacent to the quarry and are not shown on figure 11.

Table 3. Internal radial borehole displacements (μm) for typical overcore samples through specified time intervals, Barre Granite

[U_1 and U_2 are maximum and minimum displacements, positive being contraction and negative being extension]

Hole No.	Depth (m)	Internal borehole displacement		Time interval (hrs)
		principal directions		
		U_1	U_2	
3	7.02	2817	607	0
		-45	-130	21
		99	62	47
1_A	1.53	124	-163	0
		1247	-419	20
		1699	-592	40
		1834	-805	65
		2065	-920	90
		2101	-968	112
		2217	-950	135
3a	2.53	74	-79	0
		119	13	7
		2456	-2916	11
		2423	-3132	13
1_H	1.50	13	-69	0
		2383	-1803	18

¹Overcore holes A and H were drilled in surfaces adjacent to the quarry and are not shown on figure 11.

and to cool the bits. The creation of new fracture surfaces and the introduction of water to these surfaces have temporary and permanent effects on strains measured on the new surface (Savage, 1979). Several laboratory experiments were conducted to determine these effects and to determine the amount of permanent strain that may be released as a result of further dissecting the rock specimens.

The results of these experiments, too lengthy to discuss here, led to the following conclusion: Further cutting and wetting of new surfaces on granite cores, that had been stored for over a year after being removed from the intact bedrock, produced large temporary strains (500×10^{-6}) that recovered upon drying the surfaces. Permanent strains greater than 5×10^{-6} were not detected over the 18-month period following the cutting of the cores. The temporary strains were primarily a function of the available moisture and relative age of the new surface.

In summary the field data and results of the laboratory experiments reveal time-dependent deformation as great as $3200 \mu\text{m}$ and strains as great as 700×10^{-6} were measured on freshly extracted cores from the Barre Granite. Nonrecoverable strains measured after coring were on the order of 500×10^{-6} . It is concluded that much of the nonrecoverable strain measured on these cores is due to rebound and some is due to capillary absorption of moisture. Contrasting recoverable strains measured in the laboratory on specimens cut from cores after at least a year

of storage are almost entirely caused by capillary absorption and drying. The magnitude of the strains is a function of the relative humidity and the age of the new cut surface. Savage (1979) constructed a theoretical model that agreed very well with measured laboratory strains. Thus, the nonrecoverable time-dependent strains attributed to rebound seem to be short term, whereas recoverable strains of capillary absorption vary in time with relative humidity and age of surface. Longer term rebound strains are too small to be measured with the technique used here for periods of time less than a year.

Elastic Modulus Determinations

Directional Young's modulus determinations were made on specimens from or near overcore locations by sonic pulse methods and static loading methods. The sonic data presented in table 4 consist of dynamic moduli determined in three orthogonal directions: (1) perpendicular to the rift plane, (2) parallel to the rift plane and horizontal, and (3) parallel to the rift plane and vertical. Specimens used for sonic testing were taken from holes 1, 2, 1H, and 2H at or near overcore locations. Swolfs (1976) determined sonic moduli on a specimen from hole 8 (also shown in table 4). The sonic data can be compared to figures 22, 23, and 24, which show plots of static moduli determined in horizontal and vertical planes on overcore specimens taken from boreholes 1H, 2, 2H, 3, 3H, 3a, and 3s. The vertical borehole 3s, not previously mentioned, is located on an unquarried surface approximately 30 m northwest of the 67-m-high vertical quarry wall in which hole 2H is located. Determinations were made every 15° in a plane normal to the core axis. This was done by pressurizing the external surface of each annulus with a known hydrostatic pressure and monitoring displacements across the internal borehole every 15° . The USBM deformeter was used to monitor the borehole displacements. From the displacements and known applied pressures, directional moduli can be calculated in the plane of measurement. Thus, overcore annuli taken from vertical boreholes will yield moduli every 15° in the horizontal plane, and those taken from horizontal boreholes will yield moduli in a vertical plane.

Several significant patterns of modulus distributions can be seen. The data on all figures show that the granite has definite modulus anisotropies that vary in magnitude and direction. The anisotropies appear at each location to have orthorhombic symmetry. The maximum, minimum, and intermediate planar values appear to be nearly orthogonal.

The sonic-moduli values were approximately 25 percent greater than the static-moduli values and were very consistent in the common directions of measurement. Both sets of measurements showed the moduli in the N.

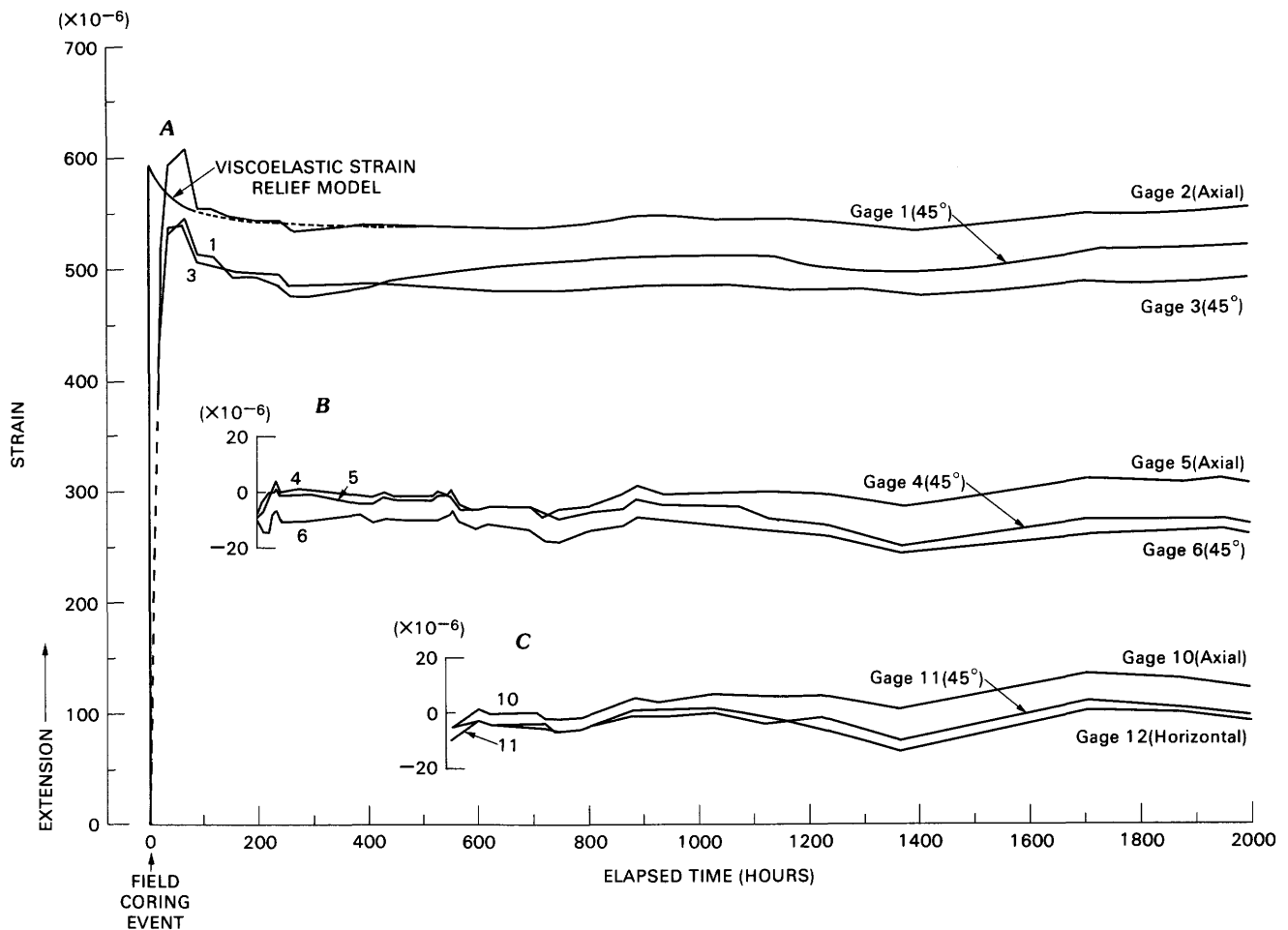


Figure 21. Strains occurring through time on a 5-cm core after extraction from drill hole 1a. Dashed line is implied from other sample measurements. Superposed curve is a theoretical viscoelastic model of strain relief based on the creep properties of the granite. Curves A, B, and C show response of strain gages mounted 4, 200, and 530 hours, respectively, after coring. Gages mounted on side of core taken from 3-m depth in drill hole.

40° E. direction to be greater than those in the N. 50° W. direction, and the vertical moduli to be intermediate.

The modulus values and distribution are important data needed for the interpretation of in situ stress measurements. In as much as Hooker and Johnson (1969) demonstrated that the effect of modulus anisotropy is small, an average value of the measured moduli is used herein for the interpretation of deformation measurements made with both the USBM and USGS borehole devices.

The following conclusions can be drawn from the moduli data.

1. On the block prior to quarrying in the active quarry area, the direction of horizontal maximum modulus does not generally coincide with the N. 40° E. direction of the rift plane (fig. 22). Only near the surface of the block did these directions tend to be parallel.

2. The maximum and minimum magnitudes of horizontal moduli, always approximately 90° apart, appear to be nearly the same at all locations in the unquarried

block. At equivalent depths, the orientations are similar but tend to change in a clockwise direction with depth. The measured vertical-moduli magnitudes were approximately equal on all cores from nearly the same depth in a horizontal hole. These were intermediate to the maximum and minimum horizontal magnitudes, thus imparting an apparent orthorhombic symmetry at these locations. Variations of vertical moduli with depth in the unquarried block were not determined.

3. The directions of maximum and minimum moduli on the block prior to quarrying do not always coincide with the respective principal stress directions. Only on the surface of the block and at 5.8-m depth do the horizontal secondary principal stress directions (table 2) coincide with the directions of maximum and minimum moduli. On the surface, the secondary major principal stress P is parallel to the minimum modulus (Swolfs, 1976), but at 5.8 m it is parallel to the maximum modulus. At 3.1-m depth, P is nearly parallel to the maximum modulus

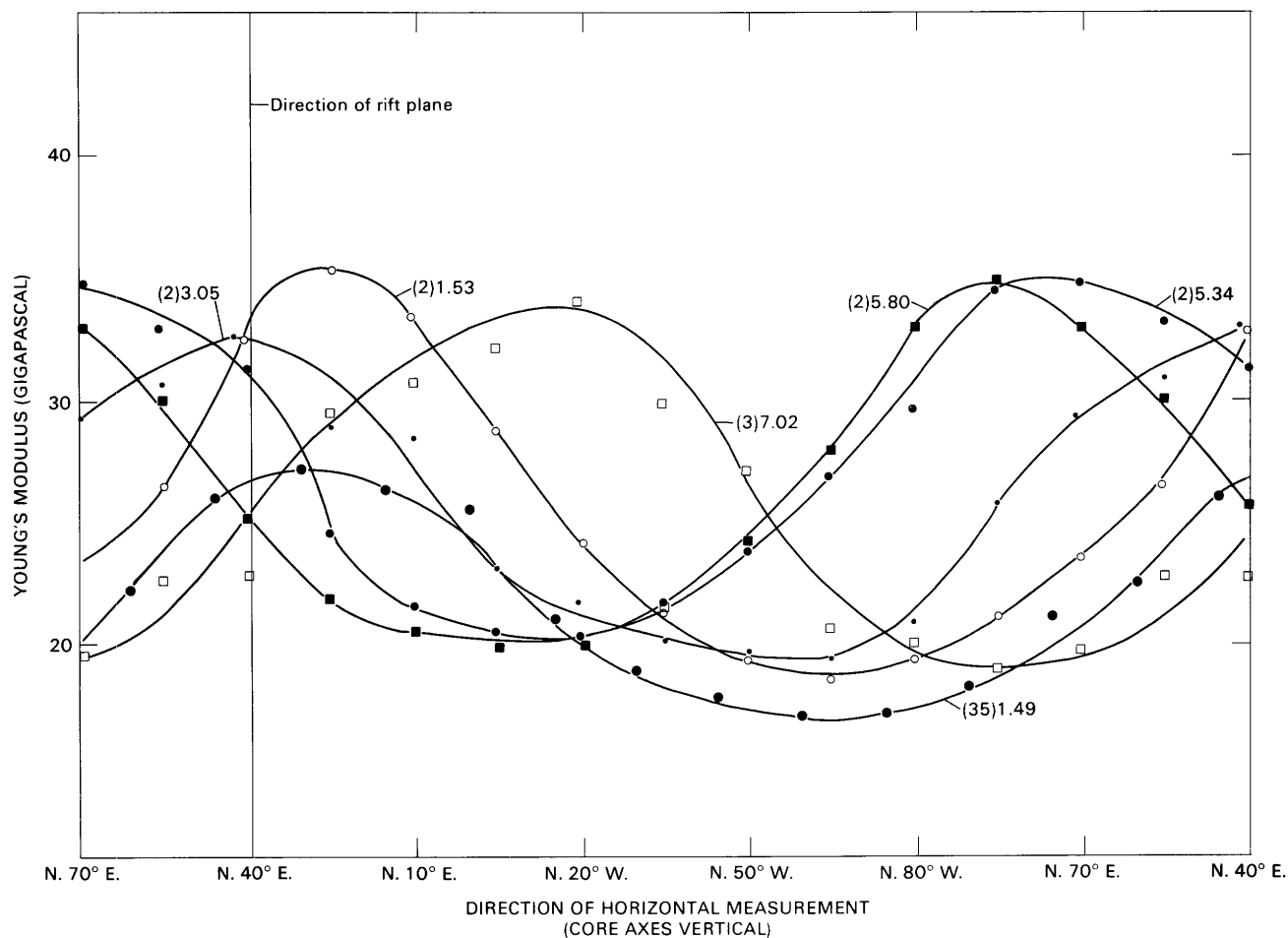


Figure 22. Variation of static Young's modulus in the horizontal plane in cores from unquarried block of Barre Granite. Curve numbers indicate borehole number in parentheses and depth in meters of cored sample used for determination.

direction. At the surface, the principal strains probably are the result of opening of microfractures in the rift plane (Swolfs, 1976; Engelder and others, 1977) where the maximum modulus is parallel to the rift plane. Below the surface, maximum strains, however, do not appear to occur primarily as the result of opening of microfractures in the rift plane.

4. The data obtained indicate that the depth of burial and degree of confinement affect the rock modulus. The modulus values of unweathered rock still under 67 m of overburden (fig. 23) are from 14 to 22 percent greater than modulus values measured in the same directions within the large quarried block (also unweathered) with only 5.7 m of overburden. On the other hand, the modulus values of rock at 1.49-m depth in the unquarried weathered rock surface (fig. 22) are 25 percent lower than those in the quarried block. The largest modulus values in the rock under 67 m overburden were in the direction of the greatest distance to a free rock surface (N. 40° E.), which was horizontal and parallel to the vertical 67-m

highwall (fig. 23). The lowest values (table 4) were in a direction of the shortest distance to a free rock surface (N. 50° W.) or normal to the 67-m highwall. Instantaneous changes of moduli were not observed as a result of rock quarrying; therefore, if changes do occur with removal of overburden they may be time dependent.

DISCUSSION OF RESULTS

The results have demonstrated that with the number and diversity of measurements, progress was made toward accomplishing the objectives of the study, but many unanswered questions remain. In retrospect, there were many problems in the logistics of the experiment; that is, the quarry geometry was less than ideal, yet the best obtainable; the geologic structure was not optimally located or oriented for an ideal experiment; and finally, not enough measurements were made to determine the distribution of data obtained. Despite these shortcomings and any possible undetermined experimental and instrument errors,

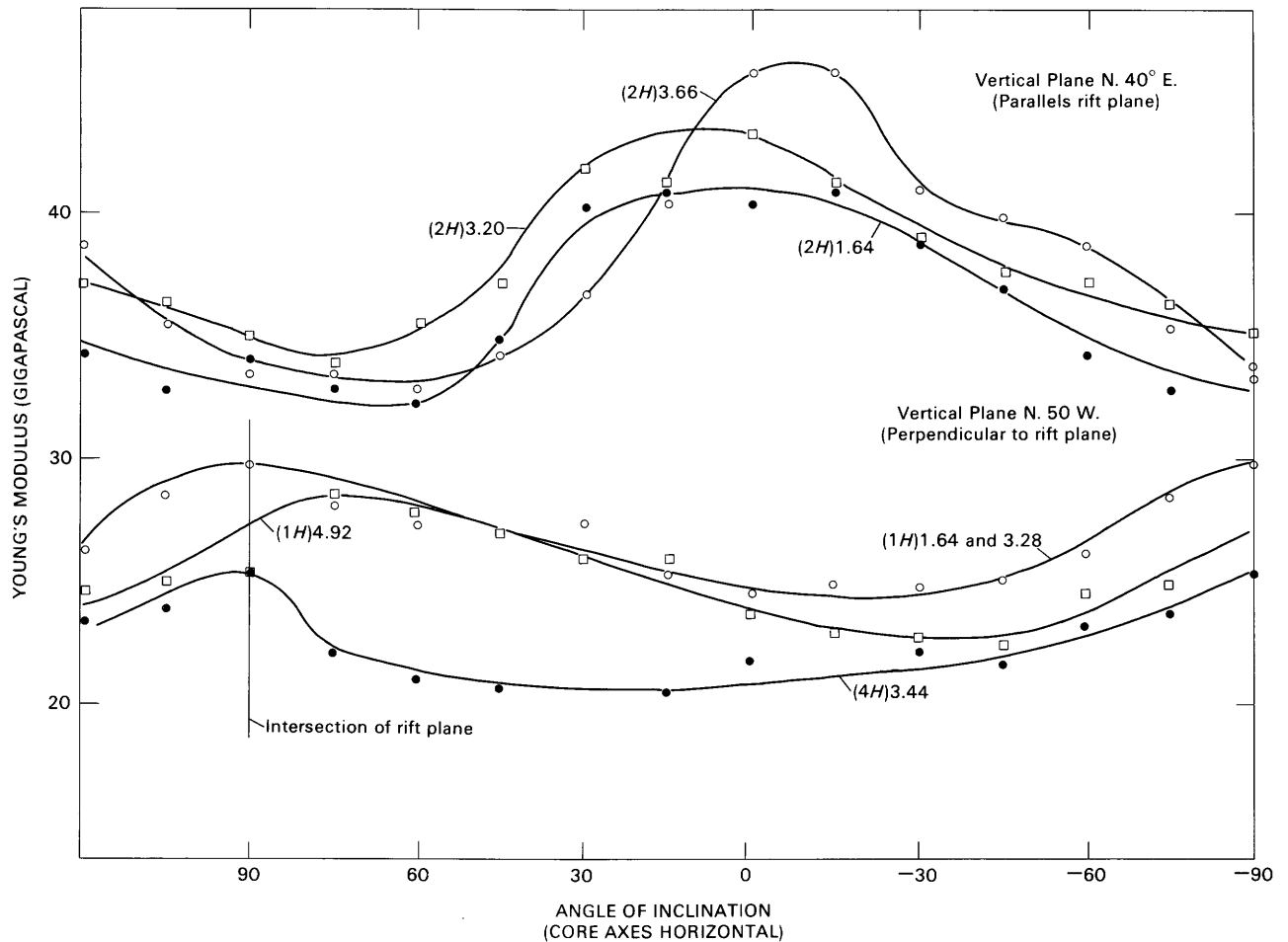


Figure 23. Variation of static Young's modulus in vertical planes striking N. 50° W. and N. 40° E. in core from unquarried block of Barre Granite. Angles are positive clockwise measured from horizontal. Curve numbers indicate borehole number in parentheses and distance in meters from surface of cored sample used for determination.

sufficient evidence exists in the data to indicate that the rock response may be in part inelastic and inappropriately used for elastic stress analyses, thereby introducing a fundamental error in interpretation.

Measurements Indicative of Inelastic-Rock Response Stress

The basic but perhaps unfounded assumption used in determining rock stresses from overcore measurements is that the recorded initial unloading rock deformations are elastic and recoverable upon reloading. Using this assumption, it is relatively easy to determine the elastic-rock constants necessary for stress calculations, merely by loading extracted overcore annuli and monitoring the elastic deformations. However, from the data obtained at Barre, there are indications that the initial unloading rock deformations measured in this process may not be dominantly elastic and therefore, may lead to stress determina-

tions with a significant error. The best evidence of nonrecoverable unloading response includes the short-term time-dependent unloading rock response measured in the field, the disk failures observed in unloaded cores, the in situ strain relaxation close to natural fractures, and the unreasonable vertical to horizontal stress distribution that is indicated in an elastic analysis of the overcore measurements.

Local Distribution of Determined Vertical and Horizontal Stress

As demonstrated, the measured strains at the Barre Granite investigation site are greatly affected less than a meter away from fractures and free surfaces. Therefore, to approximate the in situ stress distribution at our site, vertical and average horizontal stresses were determined from measurements made over 1.5 m away from such influences. The determined vertical stress components rap-

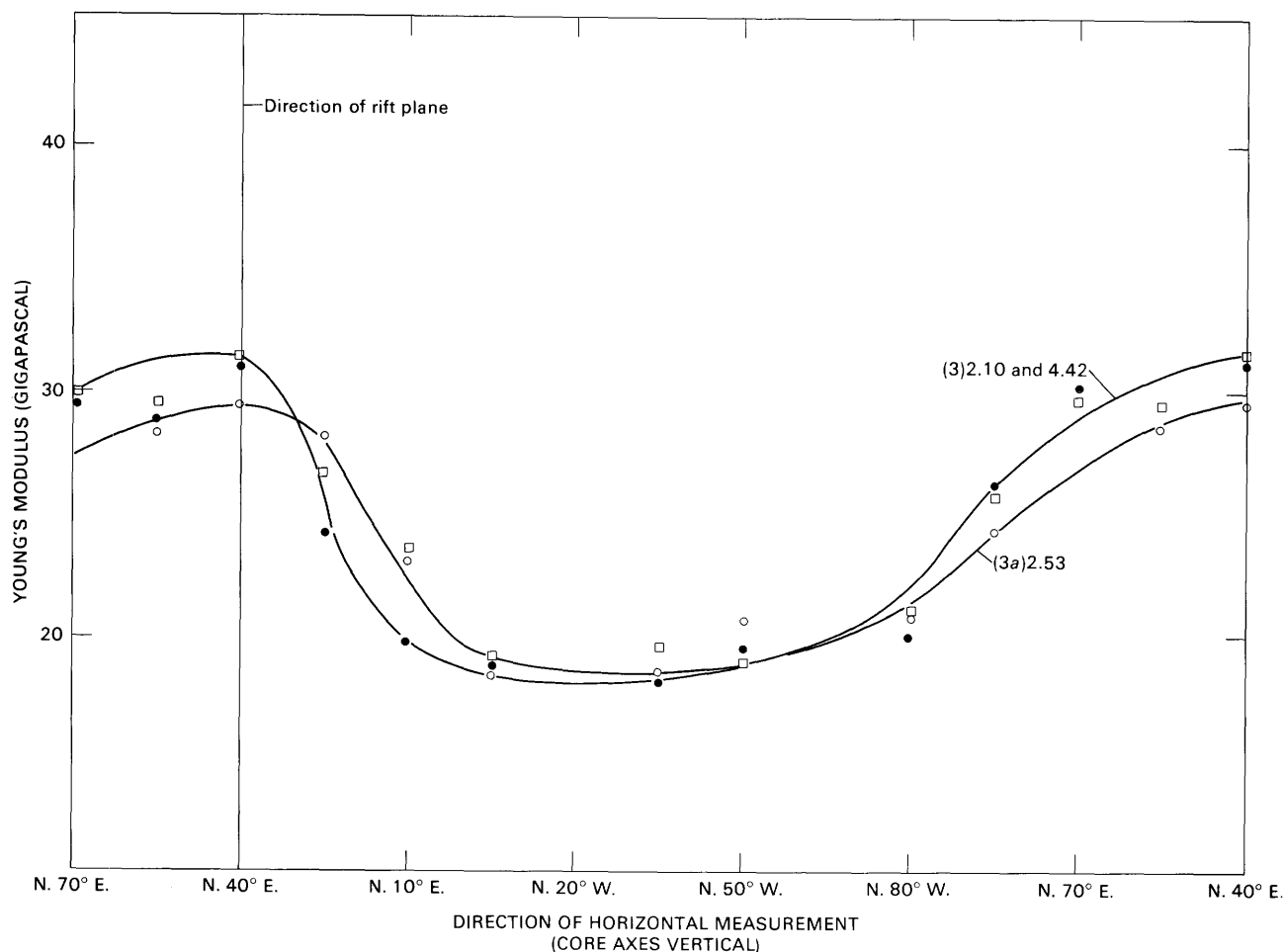


Figure 24. Variation of static Young's modulus in the horizontal plane of large quarried Barre Granite block. Curve numbers indicate borehole number and depth in meters of cored sample used for determination.

idly increase and become much greater than the gravity stress at depth, whereas the average horizontal stresses, though much larger than gravity stresses, appear to change very little at depth. Less than 6 m from the surface of the unquarried block the ratio of measured vertical stresses to the calculated vertical gravity stress $\frac{\sigma_v}{\sigma_g}$ is greater than 5. At 67-m depth in the highwall the average $\frac{\sigma_v}{\sigma_g}=5.0$. The ratio of measured average horizontal stresses (σ_h) to measured vertical stresses (σ_v), herein called K , is greater than 1 but less than 2 in the unquarried block. At 67-m depth in the highwall, K is less than 1.0 but greater than 0.4.

In this very local situation, however, it should be noted that there are insufficient measurements to establish the interpreted stress distribution with any degree of confidence, especially as it appears to be somewhat anomalous. Many more data points are needed to determine the extent and reality of the measured stress distribution. If the distribution is real and not a result of inelastic deformations,

then the impact to engineering practice and locally to quarrying becomes very significant.

Influence of Geologic Features On Determined Stress Distribution

For many years the influence of geology on in situ stress fields has been considered to be important. Mechanical behavior of geologic materials has been investigated thoroughly in the laboratory. The mechanical effects of anisotropy, discontinuities, material contrasts, environmental factors, fabric, and rheologic characteristics of geologic materials have been extensively studied (Handin and others, 1963; Donath, 1971; and Heard, 1968). However, very few attempts have been made to design field tests that demonstrate the applicability of laboratory conclusions. Notable tests are those by Swolfs and others (1974), and Lee and others (1976). The data from the Barre, Vt., experiments provide information as to how

Table 4. Young's moduli determined on cores of Barre Granite by sonic-pulse methods

[Leaders (--) indicate no data]

Location of core			Orientation of measurement		Young's modulus	
Hole No.	Depth of overburden (m)	Core distance in hole (m)	Bearing	Plunge	($\times 10^6$ psi)	(GPa)
1	0.55	0.55	N. 40° E.	0°	5.16	35.6
1	.55	.55	N. 50° W.	0°	4.13	28.5
1	.55	.55	-----	90°	4.62	31.9
1	.72	.72	N. 40° E.	0°	6.36	43.9
1	.72	.72	N. 50° W.	0°	-----	-----
1	.72	.72	-----	90°	3.70	25.5
1	1.29	1.29	N. 40° E.	0°	5.34	36.8
1	1.29	1.29	N. 50° W.	0°	3.79	26.1
1	1.29	1.29	-----	90°	4.62	31.9
2	1.53	1.53	N. 40° E.	0°	6.96	48.0
2	1.53	1.53	N. 50° W.	0°	4.41	30.4
2	1.53	1.53	-----	90°	5.53	38.1
2	3.05	3.05	N. 40° E.	0°	5.29	36.5
2	3.05	3.05	N. 50° W.	0°	4.38	30.2
2	3.05	3.05	-----	90°	4.46	30.8
2	5.34	5.34	N. 40° E.	0°	5.08	35.0
2	5.34	5.34	N. 50° W.	0°	4.62	31.9
2	5.34	5.34	-----	90°	5.25	36.2
1H	3.84	1.48	N. 40° E.	0°	5.17	35.7
1H	3.84	1.48	N. 50° W.	0°	-----	-----
1H	3.84	1.48	-----	90°	4.51	31.1
2H	67	1.53	N. 40° E.	0°	7.07	48.8
2H	67	1.53	N. 50° W.	0°	3.86	26.6
2H	67	1.53	-----	90°	5.57	38.4
8	0	----	N. 40° E.	0°	6.79	46.8
8	0	----	N. 50° W.	0°	4.50	31.0

geologic features can affect the measured in situ stress field.

Fractures and Faults

In the Barre Granite, fractures locally modify both measured stress magnitudes and orientations. The Wetmore and Morse quarry in which the USGS experiment was performed is dominated by low-angle sheeting fractures with some widely spaced tectonic fractures that have rotated into a nearly horizontal position in the vicinity of four measurements. Our measurements demonstrated that both sets affect the determined local stress field within and adjacent to the large 10×10×5.7-m block.

Most measurements affected by fractures were made near the dominant subhorizontal sheeting fractures. The effect of these fractures was to significantly relieve the vertical stress component and, to a lesser extent, to relieve the horizontal components. An excellent example of such relief is demonstrated by the stress determinations made under 67 m of overburden in horizontal hole 2H. Figure 25 depicts the locations of these measurements with re-

spect to the logged low-angle fracture. The measured components of vertical stresses and the calculated gravity stresses are shown for each location. The vertical stress component close to the fracture has been greatly relieved and nearly equals the calculated gravity stress. The horizontal stress magnitudes in the direction of maximum confinement (N. 40° E.) show no relief at any of the three locations and remain nearly the same as those in the unquarried block (table 2) under only 3–5 m of overburden.

Further, if a portion of the granite is totally separated on all sides, such as the quarried block, then nearly 95-percent stress relief occurs in all directions. Most of this relief occurs almost instantaneously, but there are continued time-dependent deformations for several days.

Evidence for Influence of Geologic History

Possibly, the geologic history of a crystalline rock mass may contribute significantly to the present-day stress field in microscopic and macroscopic domains, especially those measured stress distributions that are difficult to explain by present-day applied tectonic or gravity forces. The measured vertical-stress components (if real), the

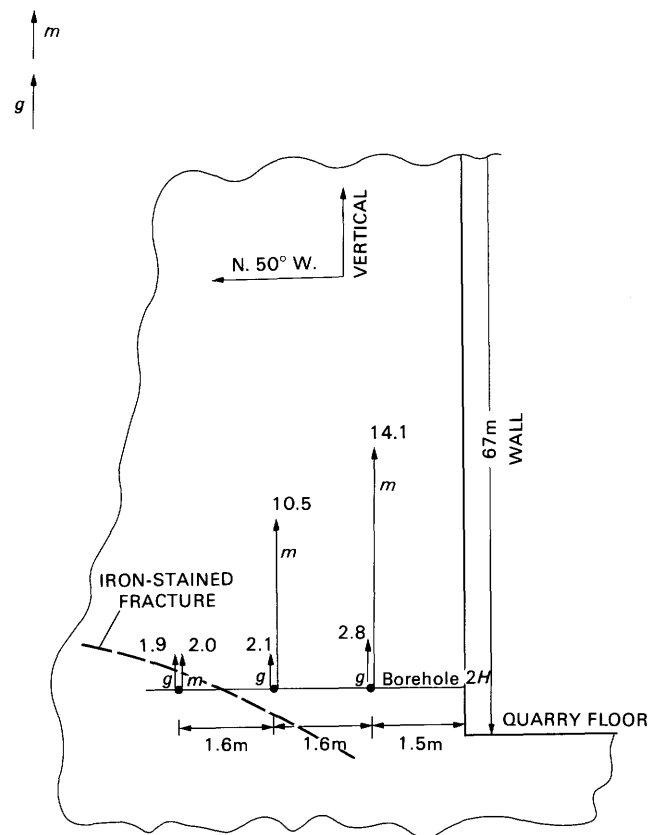


Figure 25. Vertical section through hole 2H showing locations of overcores and a natural fracture. Vectors at each location show measured vertical stresses (m) and calculated gravity stresses (g) from table 2. Values are Megapascals.

time-dependent response, the stress relief near fractures, and the release of strain perpendicular to the rift plane may be a response to stress fields created by past geological processes. There is fabric- and mechanical-behavior evidence that changes in elastic properties also may be caused by long-term relief of paleostress fields.

The crystalline rocks listed herein have all undergone thermal changes as a result of burial, denudation, and tectonic forces. The Barre Granite has undergone significant brittle and ductile deformation as a result of intrusion and cooling, which is reflected in the rock fabric.

Fabric

As pointed out previously, the Barre Granite has a dominant microscopic fabric that includes strongly developed open microfractures within quartz grains in a nearly vertical planar trend striking about N. 30°–70° E. Strong macroscopic fabrics can be seen in the well developed but apparently different fracture systems of the upper and lower quarry areas (fig. 5).

The microfracture fabric that pervades the Barre Granite in quarried areas may have been formed as a result of one or possibly two cooling stages within a deviatoric stress field that existed during the time of fracturing. Nur and Simmons (1970) attributed the development of microcracks to large shear stresses at grain boundaries caused by differential thermal strains upon the cooling of rock masses. Savage (1978) demonstrated that under a hydrostatic state of stress, tensile stresses on the order of 480 MPa are developed and stored in quartz grains (compared to compressive stresses of about 159 MPa in the feldspar grains) within an idealized granite by cooling the granite through 300°C. If stresses of this magnitude existed on a grain to grain basis within the Barre pluton, they are certainly sufficient to cause tensile failure and some relaxation in the quartz crystals. If a stress field, such as that required to create the northeast-trending fracture system (p. 12), is superposed on Savage's idealized hydrostatic cooling model, the tensile fractures in the quartz grains would have a strong preferred orientation. For instance, suppose that the pluton was still buried to a depth of 10 km and had cooled from about 500° to 200°C, but was under an external stress field where σ_3 was horizontal and approximately 75 MPa. The melting temperature of a water-saturated granite at a depth of 10 km is about 700°C (Verhoogen and others, 1970, p. 278, 658), and the Precambrian shield geotherm at the same depth is less than 200°C; therefore, the chosen cooling temperatures seem reasonable. In addition, the cooling time (Verhoogen and others, 1970, p. 588) for the size of the pluton (4-km diameter) appears to be less than 1 million years, which also seems reasonable. At this depth, σ_3 acting in the horizontal plane may be estimated to be that caused by the weight of overburden, 75 MPa, if the

rock is considered to be elastic. The estimated σ_3 is calculated using the equation $\sigma_h = (\frac{\nu}{1-\nu}) \sigma_v$, from elastic theory, letting Poisson's ratio $\nu=0.25$ and the vertical stress, $\sigma_v=225$ MPa. Under these conditions the largest tensile stress component in the quartz resulting from the superposition of the cooling stresses would be about 405 MPa, and microcracks could develop normal to this direction. If the rock adjusted through creep to a lithostatic stress condition prior to cooling and σ_3 approached the vertical stress of 225 MPa, the resulting tensile stress component in the quartz would be 255 MPa, which is still sufficient for tensile failure. Effective stresses, based on hydrostatic pore pressures would allow even more tensile stress in the quartz. In support of this argument, quartz grains in thin sections are seen to have open tensile microcracks with a preferred orientation of approximately N. 40° E. (fig. 10). Bubble planes in quartz grains, evidence of healed microfractures oriented about N. 70° E., can be seen in the thin sections, indicating a possible rotation of the minimum principal paleostress axes of about 30° in the horizontal plane. The bubble planes indicate that the granite has gone through at least one reheating event in which the oldest microfractures have been healed or annealed. The microscopic fabric of the Barre Granite is evidence that supports Savage's microscopic model as a viable one, allowing large thermally induced stresses to be stored on the very local grain-to-grain basis.

On a much larger scale, macrofabric such as the vertical tectonic fractures in the upper quarries and the well-developed shear zones that dominate the lower quarries also illustrate the influence of past tectonic history. As previously discussed, a paleotectonic stress field with sufficiently large magnitude shear stresses to create these features probably was transmitted across the pluton during the cooling stages of the granite. In addition, a thermoelastic stress field caused by the cooling of the pluton was probably superposed and stored in the pluton. On this larger scale Savage (1978) also demonstrated that radial stresses may be stored uniformly across an ideal spherical pluton when cooled in a hydrostatic stress field. The magnitude of stresses he calculated for a pluton similar in composition to the Barre Granite, surrounded by metamorphic rocks, was 23.2 MPa in compression, which is somewhat larger than those measured in this experiment.

Relief of the pluton through uplift and erosion has occurred only on the top surface which represents a very small fraction of the nearly totally confined volume of granite extending below the surface. Therefore, because of this limited relief, it is reasonable to believe that if cooling stresses of the magnitude calculated by Savage existed in the Barre Granite, the present-day measured stress field may be attributed to this phenomenon and the superposed present-day gravity stress field.

Relief Characteristics

The distribution of measured deformations away from fractures and free surfaces illustrates the manner in which stress in the Barre Granite becomes relieved at fracture surfaces. Note again that all of the vertical-stress determinations made less than 0.5 m from a sheet fracture agree with the calculated gravity stress curve, indicating that only the weight of the overlying rocks was measured. For those data taken more than 1 m from a sheet fracture, the interpreted vertical stresses increase at depth, becoming much greater than the calculated gravity stresses and somewhat greater than the horizontal stresses. If these stresses are not a result of erroneous interpretation resulting from inelastic deformations, it is possible that the stress field resulting from the cooling of the granite left its imprint. The fact that observed vertical deformations appear to increase significantly with depth and distance away from sheeting fractures, whereas horizontal deformations increase only slightly with depth and diminish only when very close to sheeting fractures, may be a function of vertical unloading of the combined thermoelastic and gravity stress field by erosion. The degree of horizontal unloading by erosional processes is considerably less than vertical unloading; thus, horizontal stresses have a much smaller gradient with depth. The smaller horizontal gradient is consistent with gravity loading in a rock mass that is laterally perfectly constrained, where the increase of horizontal gravity stress (σ_h) can be approximately related to the vertical gravity stress (σ_v) by the relationship $\sigma_h = \left(\frac{\nu}{1-\nu}\right)\sigma_v$. If a uniform thermoelastic cooling stress (σ_t) of unknown magnitude and gradient is superposed upon the gravity stress, then the relationship becomes $\sigma_h + \sigma_{th} = \left(\frac{\nu}{1-\nu}\right)\sigma_v + \sigma_{th}$ where σ_{th} is the horizontal component of the thermoelastic stress. The total horizontal stress becomes $\sigma_h = \left(\frac{\nu}{1-\nu}\right)\sigma_v + \sigma_{th}$ and in the same manner the total vertical stress becomes $\sigma_v = \sigma_v + \sigma_{tv}$. Using calculated values of σ_h and σ_v , estimated values of σ_{th} and σ_{tv} based on our data, and $\nu=0.25$ in the above relationship gives

1. At 3-m depth: $\sigma_v=0.06$ MPa, $\sigma_h=0.02$ MPa, $\sigma_{tv}\approx 1.6$ MPa, $\sigma_{th}\approx 6.5$ MPa. $\sigma_h\approx 6.52$ MPa, $\sigma_v\approx 1.66$ MPa
2. At 67-m depth: $\sigma_v=1.5$ MPa, $\sigma_h=0.5$ MPa, $\sigma_{tv}\approx\sigma_{th}\approx 9.0$ MPa, $\sigma_h\approx 9.5$ MPa, $\sigma_v\approx 10.5$ MPa

These figures are close enough to the measured values to demonstrate that a large-volume thermoelastic stress field, relieved only near the surface and superposed on a gravity stress field, may be a reasonable explanation of the total stress field.

In addition, stresses in the large block at Barre appeared to be completely relieved after quarrying, except for time-dependent deformations that continued over a period of 10 days after quarrying. Thus, the volume of

the block is smaller than the rock volume subjected to the applied stress field indicating the existence of a large-volume viscoelastic paleostress field.

The relief characteristics to a depth of 67 m suggest the possibility that a gravity stress field is superposed on a large-volume thermoelastic stress field. This superposition results in a vertical stress component much larger than gravity that increases significantly to 67 m compared to a horizontal component that may show only a small increase to this depth. At 67-m depth, the vertical component is larger than the horizontal component. A stress field of this nature may be supported by the geologic thermoelastic history of the pluton.

Modulus

Elastic theory predicts that in ideal materials stress is directly related to strain through the modulus. As discussed above, in the Barre Granite there are significant variations of modulus with depth and fabric anisotropy that can only be related to the measured stress levels in a general way.

Young's modulus values have been computed from measurements made on various cores retrieved from core holes. Though no field measurements were made that could be used to adequately determine the in situ Young's modulus, the laboratory data obtained demonstrated that the rock moduli increased with sample depth and decreased with elapsed time since removal of the overburden. A decrease of rock modulus occurs as a result of erosion or excavation of the overburden and likely is a result of inelastic creep deformation caused by the opening of fractures and further enhanced by chemical weathering processes.

As previously stated, the moduli increased with depth; also the orientations of maximum stiffness, parallel to the rift plane only at the surface, tended to change in a counterclockwise direction with depth. For stress measurements made below 3 m, the determined secondary major stress direction P was nearly parallel to the maximum modulus direction, whereas at the surface P was perpendicular to this direction. Geologic controls for the variation of maximum stiffness orientations with depth are not known, but should be investigated. It is possible that the directions and magnitudes of stiffness may vary merely as a function of changing preferential directions of microcrack opening as overburden loads are removed by erosion. This phenomenon was alluded to by Farrow (1973) when he demonstrated that a laboratory specimen of Mount Airy Granite, when repeatedly hydrostatically loaded to 34.5 MPa, changed the elastic principal strain orientations $\Delta\epsilon_1$, and $\Delta\epsilon_2$, by approximately 90°, thereby implying an identical recoverable change in the stiffness directions. He interpreted these changes to be a result of differential microfracture closure.

Thus, the quarrying operations as well as natural erosional processes may have considerable effect on the stiffness variations within the rock mass at this location and therefore affect the measured state of stress. The dominant observed microcrack fabric appears to be a controlling factor only near the surface, where the removal of confinement has allowed the opening of these cracks. The unloading history of the granite then appears to be significant to the orientation as well as magnitude of the in situ stress field.

SIGNIFICANCE OF BARRE DATA TO QUARRYING AND ENGINEERING PRACTICE

In the Barre quarries, the quarrying conditions are less than ideal. In the vicinity of our experiment, commercial-grade rock is commonly lost, because it fails prior to or because of extraction (fig. 26). The incidence of failures increases with the depth of quarrying.

The data from Barre contribute only in a general way to the understanding of these failures and raise additional questions that remain unanswered. If the vertical stress gradient does increase with depth relative to the horizontal as the data indicate, then quarrying at increased depths would tend to greatly enhance vertical displacements on the quarry floor that give rise to sheet fractures. However, the fractures do not always develop instantaneously as overburden is stripped away, so the displacements causing failure often are time dependent, indicating a viscoelastic response or a time-dependent readjustment of the stress field. Disking of cores taken from the quarried $10 \times 10 \times 5.7$ -m block, described on p. 38, is a failure of this nature.

The other tensile failures on the corners and edges of partially quarried blocks also were time dependent and within a locally relieved portion of the rock. Deformation measurements were not made on these boundaries to determine displacements leading to failure, but other measured displacements on the side of the quarried block and on extracted core samples show comparatively large extensional strains for days after being relieved, indicating a viscoelastic response sufficient to cause tensile failure.

The failures described here no doubt are affected by the quarry geometry. If the depth to width ratio (D/W) is relatively large and becomes increasingly large with depth of quarrying, the unusually high measured vertical-deformation gradient may continue to increase and cause significant damage to the quarry floor. Whereas, if D/W is kept relatively low, the vertical gradient could be partially relieved. This would mean the quarrying would have to be broadened as well as deepened.

For engineering practice, the results presented herein may be of consequence to the design practices for large

excavations. Useful design criteria to allow enhanced excavation stability and integrity of quarried blocks depend on obtaining reliable information of stress distribution, time-dependent rebound of the excavated rock, and rock temperature variations, as well as observations of failure modes. In addition, the data observed at Barre indicate the possibility of rock strength decreasing with time. Depending on the design life of the excavation, this factor may be important and should also be studied.

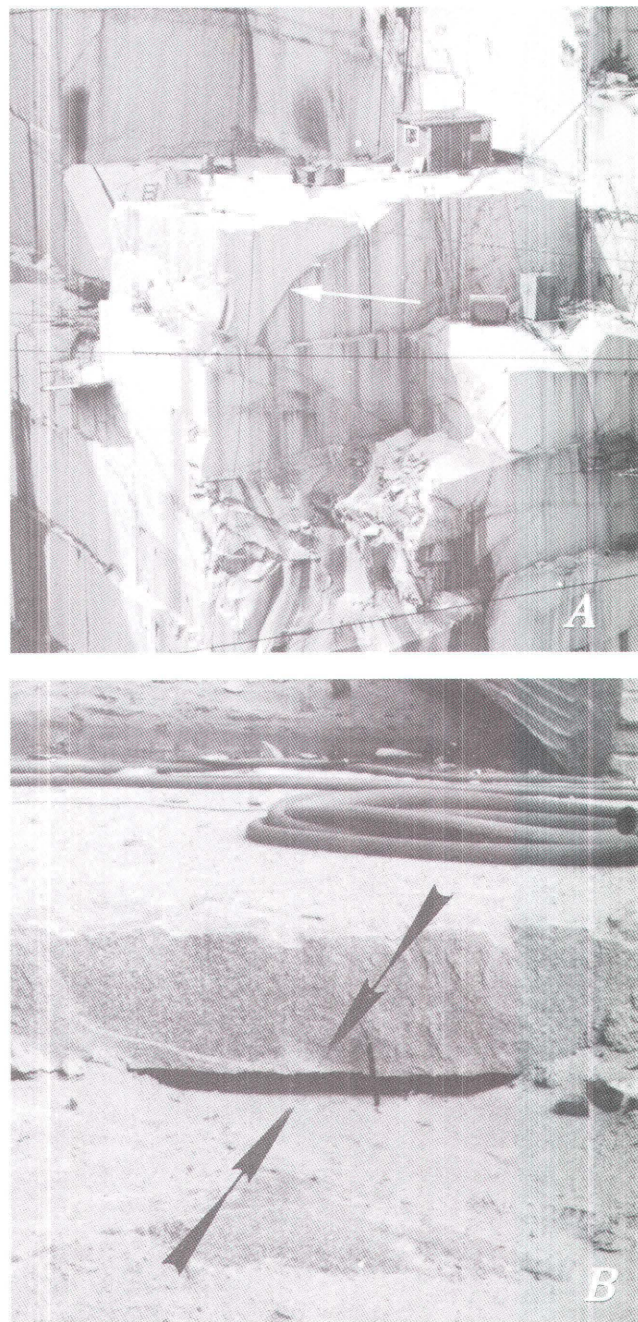


Figure 26. Fractures at edges of partially freed granite blocks (A), and in bottom of quarry (B), Barre, Vt.

Finally, the deformation measurements may be most useful without attempting to determine the associated stress field. The interpreted stress magnitudes stated herein are questionable, whereas the deformation measurements used for the interpretation are judged to be of good quality. In order to make more reliable stress determinations, additional work must be done in evaluation of the degree of elastic versus inelastic response of rock masses when the in situ constraints are removed.

CONCLUSIONS

Shallow stress measurements in the Barre Granite of Vermont demonstrate that locally the determined stress distribution cannot be explained wholly by gravity or present-day tectonic loading. Tectonic forces may explain the horizontal loads, but past thermoelastic loads caused by cooling of rocks may possibly explain both the horizontal and excess vertical loads. The geologic history and associated thermoelastic stresses may explain the magnitudes and directions of stresses in geologic terranes such as the Barre Granite. Work done in the unloading of such a stress field by the removal of external loads results in viscoelastic recovery and the subsequent development of fractures resulting from extensional strains. On the other hand, it is quite possible that the interpreted stresses are in error because a significant component of the measured deformations are inelastic rather than elastic. In either case, unloading by natural erosional processes results in the formation of sheeting fractures, whereas unloading by quarrying results in the formation of extensional fractures on edges and free surfaces of the partially quarried granite outcrops.

The viscoelastic responses can be critical to good quarrying procedure and to the stability of engineering excavations and installations, especially those that are designed for long-term use. Thus, it is very important to analyze in situ stress or strain fields and deformations resulting from the removal of rock masses in the crystalline terranes, in order to develop constitutive relations and failure criteria that can be used for design purposes.

REFERENCES

- Balk, Robert, 1937, Structural behavior of igneous rocks: Geological Society of America Memoir 5, 177 p.
- Cady, W. M., 1960, Stratigraphic and geotechnic relationships in northern Vermont and southern Quebec: Geological Society of America Bulletin, v. 71, no. 5, p. 531–576.
- Chayes, Felix, 1952, The finer grained calc-alkaline granites of New England: Journal of Geology, v. 60, p. 207–254.
- Currier, L. W., and Jahns, R. H., 1941, Ordovician stratigraphy of central Vermont: Geological Society of America Bulletin, v. 52, p. 1487–1512.
- Dale, T. N., 1909, The granites of Vermont: U.S. Geological Survey Bulletin 404, 135 p.
- 1923, Commercial granites of New England: U.S. Geological Survey Bulletin 738, 488 p.
- Doll, C. G., 1943, A Paleozoic revision in Vermont: American Journal of Science, v. 241, p. 57–64.
- 1951, Geology of the Memphremagog quadrangle and the southeastern portion of the Irasburg quadrangle, Vermont: Vermont Geological Survey Bulletin 3, 113 p.
- Donath, F. A., Faill, R. T., and Tobin, D. G., 1971, Deformational mode fields in experimentally deformed rocks: Geological Society of America Bulletin, v. 82, no. 6, p. 1441–1462.
- Durelli, A. J., Obert, Leonard, and Parks, V. J., 1968, Stress required to initiate core discing: Society of Mining Engineers Transactions, v. 241, p. 269–271.
- Engelder, Terry, Sbar, M. L., and Kranz, Robert, 1977, A mechanism for strain relaxation of Barre Granite—opening of microfractures: Pure and Applied Geophysics, v. 115, p. 27–40.
- Farrow, R. A., 1973, A new method for the determination of three-dimensional deformation anisotropy in rock specimens: U.S. Geological Survey Bulletin 1258-E, 12 p.
- Faul, Henry, Stern, T. W., Thomas, H. H., and Elmore, P. L. D., 1963, Ages of intrusion and metamorphism in the northern Appalachians: American Journal of Science, v. 261, p. 1–19.
- Finlay, G. I., 1902, The granite area of Barre, Vermont: Vermont State Geologist, 3d Report, p. 46–59.
- Handin, John, Hager, R. V., Jr., Friedman, Melvin, and Feather, J. N., 1963, Experimental deformation of sedimentary rocks under confining pressure—Pore pressure tests: American Association of Petroleum Geologists Bulletin, v. 47, no. 5, p. 717–755.
- Heard, H. C., 1968, Experimental deformation of rocks and the problem of extrapolation to nature, in Riecker, R. E., NSF Advanced Seminar in Rock Mechanics: Boston College, v. 2, p. 439–508.
- Hooker, V. E., and Bickel, D. L., 1974, Overcoring equipment and techniques: U.S. Bureau of Mines Progress Report DMRC 10002, 29 p.
- Hooker, V. E., Bickel, D. L., and Aggson, J. R., 1972, In situ determination of stresses in mountainous topography: U.S. Bureau of Mines Report of Investigations 7654, 19 p.
- Hooker, V. E., and Duvall, W. I., 1971, In situ rock temperature stress investigations in rock quarries: U.S. Bureau of Mines Report of Investigations 7589, 12 p.
- Hooker, V. E., and Johnson, C. F., 1969, Near-surface horizontal stresses including the effects of rock anisotropy: U.S. Bureau of Mines Report of Investigations 7224, 29 p.
- Lee, F. T., Abel, J. F., Jr., and Nichols, T. C., Jr., 1976, Stress changes caused by excavation, Idaho Springs, Colorado: U.S. Geological Survey Professional Paper 965, 47 p.
- Murthy, V. R., 1957, Bedrock geology of the East Barre area, Vermont: Vermont Geological Survey Bulletin 10, 121 p.
- Naylor, R. S., 1971, Acadian orogeny—an abrupt and brief event: Science, v. 172, no. 3983, p. 558–560.

- Nichols, T. C., Jr., 1975, Deformations associated with relaxation of residual stresses in a sample of Barre Granite from Vermont: U.S. Geological Survey Professional Paper 875, 32 p.
- 1980, The state of stress in the Barre Granite of Vermont, and other near-surface rocks of North America—Paleo and present-day stress fields and the significance to engineering practice: Boulder, Colorado, University of Colorado, Ph. D. thesis, 196 p.
- Nichols, T. C., Jr., and Savage, W. Z., 1976, Rock strain recovery; factor in foundation design: *in* Rock engineering for foundations and slopes; Proceedings of a specialty conference, American Society of Civil Engineers, New York, N. Y., v. 1 (Anonymous), p. 34–50.
- Nichols, T. C., Jr., Savage, W. Z., and Brethauer, G. E., 1977, Deformations and stress changes that result from quarrying the Barre Granite of Vermont, *in* Energy and mineral resource recovery, ANS Topical Meeting, Golden, Colorado, 1977: U.S. Department of Energy, p. 791–803.
- Nur, Amos, and Simmons, Gene, 1970, The origin of small cracks in igneous rocks: *International Journal of Rock Mechanics and Mining Sciences*, v. 7, no. 3, p. 307–315.
- Savage, W. Z., 1978, The development of residual stress in cooling rock bodies: *Geophysical Research Letters*, v. 5, no. 8, p. 633–636.
- 1979, A model of the strain response of Barre Granite to wetting and drying: U.S. Geological Survey Open-File Report 79–768, 17 p.
- Shelton, K. L., and Orville, P. M., 1980, Formation of synthetic fluid inclusions in natural quartz: *American Mineralogist*, v. 65, nos. 11 and 12, p. 1233–1236.
- Simmons, Gene, and Richter, Dorothy, 1976, Microcracks in rocks, *in* Strens, R. G. J., The physics and chemistry of minerals and rocks: New York, Wiley-Interscience, p. 105–137.
- Sokolnikoff, I. S., 1956, *Mathematical theory of elasticity*: New York, McGraw-Hill, 476 p.
- Swolfs, H. S., 1976, Field investigation of strain relaxation and sonic velocities in Barre Granite, Barre, Vermont: Terratek Final Report TR 76–13, 13 p.
- Swolfs, H. S., Handin, J., and Pratt, H. R., 1974, Field measurements of residual strain in granitic rock masses: *International Society of Rock Mechanics Congress*, 3d, Denver, Colorado, Proceedings, v. 2, pt. A, p. 563–568.
- Thill, R. E., Bur, T. R., and Steckley, R. C., 1973, Velocity anisotropy in dry and saturated rock spheres and its relation to rock fabric: *International Journal of Rock Mechanics and Mining Sciences*, v. 10, no. 6, p. 535–558.
- Tullis, Jan, and Yund, R. A., 1977, Deformation behavior of quartz and feldspar in experimentally deformed granite: *Journal of Geophysical Research*, v. 82, p. 5705–5718.
- Verhoogen, John, Turner, F. J., Weiss, L. E., and Wahrhaftig, Clyde, 1970, *The earth, an introduction to physical geology*: San Francisco, Holt, Rinehart, and Winston, 748 p.
- White, W. S., and Jahns, R. H., 1950, Structure of central and east-central Vermont: *Journal of Geology*, v. 58, no. 3, p. 179–220.
- Willard, R. J., and McWilliams, J. R., 1969, Microstructural techniques in the study of physical properties of rock: *International Journal of Rock Mechanics and Mining Sciences*, v. 6, p. 1–12.
- Zartman, R. E., Hurley, P. M., Krueger, H. W., and Giletti, B. J., 1970, A Permian disturbance of K-Ar radiometric ages in New England—its occurrence and cause: *Geological Society of America Bulletin*, v. 81, no. 11, p. 3359–3374.

